Rif2 protects Rap1-depleted telomeres from MRX-mediated degradation in *Saccharomyces cerevisiae*

Fernando R. Rosas Bringas[1], Sonia Stinus[1], Pien de Zoeten[1], Marita Cohn[2], and Michael Chang[1,*]

[1]European Research Institute for the Biology of Ageing, University of Groningen, University Medical Center Groningen, Groningen, The Netherlands

[2]Department of Biology, Lund University, Lund, Sweden

[*]For correspondence: m.chang@umcg.nl

Abstract

Rap1 is the main protein that binds double-stranded telomeric DNA in *Saccharomyces cerevisiae*. Examination of the telomere functions of Rap1 is complicated by the fact that it also acts as a transcriptional regulator of hundreds of genes and is encoded by an essential gene. In this study, we disrupt Rap1 telomere association by expressing a mutant telomerase RNA subunit (tlc1-tm) that introduces mutant telomeric repeats. *tlc1-tm* cells grow similar to wild-type cells, although depletion of Rap1 at telomeres causes defects in telomere length regulation and telomere capping. Rif2 is a protein normally recruited to telomeres by Rap1, but we show that Rif2 can still associate with Rap1-depleted *tlc1-tm* telomeres, and that this association is required to inhibit telomere degradation by the MRX complex. We find that Rap1, Rif2, and the Ku complex work in parallel to prevent telomere degradation, and absence of all three at telomeres causes lethality. The partially redundant mechanisms may explain the rapid evolution of telomere components in budding yeast species.

Keywords: Rap1, Rif2, Ku complex, telomere, telomerase, tlc1-tm, yeast

Introduction

Telomeres, nucleoprotein complexes located at the ends of eukaryotic chromosomes, protect chromosome ends from degradation, from telomere-telomere fusion events, and from being recognized as double-stranded DNA breaks (Wellinger & Zakian, 2012; de Lange, 2018). In most eukaryotic species, telomeric DNA consists of tandem G/C-rich repeats of double-stranded DNA with the G-rich strand extending to form a 3′ single-stranded overhang. These repeats are bound by specialized proteins—some to the double-stranded region and others to the 3′ overhang—which are important for proper telomere function. Telomere length is maintained by a dynamic process of shortening and lengthening. Telomeres shorten due to incomplete DNA replication and nucleolytic degradation, and are lengthened by the action of a specialized reverse transcriptase called telomerase (Wellinger, 2014). At its core, telomerase consists of a catalytic protein subunit and an RNA subunit, and extends telomeres by iterative reverse transcription of a short G-rich sequence to the 3′ overhang, using the RNA subunit as a template.

Rap1 is the main double-stranded telomeric DNA binding protein in the budding yeast *Saccharomyces cerevisiae* (Buchman et al., 1988; Conrad et al., 1990), with important roles in regulating telomere length (Lustig et al., 1990; Conrad et al., 1990; Marcand et al., 1997), transcriptional silencing of subtelomeric genes (Kyrion et al., 1993), and preventing telomere-telomere fusions (Pardo & Marcand, 2005). Rap1 mediates these functions in part by recruiting additional proteins (i.e. Rif1, Rif2, Sir3, and Sir4) via its C-terminal domain (Hardy et al., 1992; Wotton & Shore, 1997; Moretti et al., 1994). Expression of a mutant Rap1 lacking the C-terminal domain, which retains the ability to bind telomeric sequences, mimics the deletion of the *RIF* and *SIR* genes in terms of telomere length regulation and subtelomeric gene silencing (Wotton & Shore, 1997; Kyrion et al., 1993). However, the telomeric functions of Rap1 are not limited to the recruitment of Rif and Sir proteins. For

54 example, although Rif2 and Sir4 are important for the inhibition of telomere end-to-end
55 fusions, Rap1 also inhibits fusions independently of Rif2 and Sir4 (Marcand et al., 2008). In
56 addition, binding of Rap1 to telomeric repeats is thought to promote replication fork pausing
57 and breakage of dicentric chromosomes at telomere fusions independently of the Rif and Sir
58 proteins (Makovets et al., 2004; Guérin et al., 2019; Douglas & Diffley, 2021). Despite the
59 central role of Rap1 in yeast telomere biology, its study is complicated by the fact that Rap1
60 is also a transcription factor that regulates the expression of a few hundred genes (Lieb et al.,
61 2001). Moreover, *RAP1* is essential for viability (Shore & Nasmyth, 1987), preventing
62 analysis of a gene deletion mutant.

63 In this study, we examined the function of Rap1 at *S. cerevisiae* telomeres by
64 expressing a mutant telomerase RNA subunit (tlc1-tm) that introduces $[(TG)_{0-}$
65 $_{4}TGG]_{n}ATTTGG$ mutant telomeric repeats instead of wild-type $(TG)_{0-6}TGGGTGTG(G)_{0-1}$
66 repeats (Chang et al., 2007; Förstemann & Lingner, 2001). We find that Rap1 binds very
67 poorly to mutant telomeric sequences, yet *tlc1-tm* cells are viable and grow similar to wild-
68 type cells. The depletion of Rap1, not surprisingly, causes telomere length homeostasis
69 defects. Unexpectedly, the overall levels of Rif2 at telomeres are unaffected. Rif2 recruitment
70 to *tlc1-tm* telomeres is dependent on the MRX complex, and Rif2 is crucial for preventing
71 *tlc1-tm* telomeres from degradation by the MRX complex. The yeast Ku complex functions
72 in parallel to protect *tlc1-tm* telomeres, and absence of both Rif2 and the Ku complex renders
73 *tlc1-tm* cells inviable. Our findings reveal multiple redundant mechanisms that may have
74 been important for the rapid evolution of telomere components in budding yeasts.
75

76 ## Results

77 **Rap1 binds poorly to *tlc1-tm* sequences**

78 To examine the function of Rap1 specifically at telomeres, we made use of a telomere RNA
79 mutant, *tlc1-tm*. Rap1 has a consensus DNA binding sequence of 5′-CACCCAYACMYM-3′
80 (where Y is C or T, and M is A or C) containing an invariable CCC core (Graham &
81 Chambers, 1994; Lieb et al., 2001). The template region of wild-type TLC1 is 3′-
82 CACACACCCACACCAC-5′, resulting in the addition of $(TG)_{0\text{-}6}$TGGGTGTG$(G)_{0\text{-}1}$
83 telomeric repeats (Förstemann & Lingner, 2001). The tlc1-tm template region is 3′-
84 CACCUAAACCACACAC-5′, resulting in $[(TG)_{0–4}TGG]_n$ATTTGG mutant telomeric
85 repeats (Chang et al., 2007). The lack of the GGG motif in the mutant repeat sequence should
86 disrupt Rap1 binding, yet the *tlc1-tm* mutant grows similar to a wild-type strain (Fig. 1A).
87 Telomeres in the *tlc1-tm* mutant are on average longer and more heterogeneous in length than
88 in wild-type strains (Fig. 1B), but the telomere profile of *tlc1-tm* is much less dramatically
89 altered compared to most other *TLC1* mutants with altered template sequences (Förstemann
90 et al., 2003; Lin et al., 2004). Telomeres in *tlc1-tm* cells were previously reported to be
91 slightly shorter than in wild-type cells, as measured by telomere PCR (Chang et al., 2007).
92 This discrepancy is likely due to the tendency of PCR to amplify shorter fragments more
93 efficiently that longer ones.
94 Because telomerase only adds repeats to the distal end of telomeres, the proximal
95 region of *tlc1-tm* telomeres still contains some wild-type repeats with the capacity to be
96 bound by Rap1. Thus, we engineered strains in which the left arm of chromosome VII (VII-
97 L) ends with a telomere that consists entirely of either wild-type or *tlc1-tm* telomeric
98 sequence (Fig. 1C). These strains were constructed by replacing the native VII-L telomere
99 with the *URA3* gene followed by 81 bp of wild-type or 84 bp of *tlc1-tm* telomeric seed
100 sequence, which was lengthened in vivo by either wild-type or *tlc1-tm* mutant telomerase,
101 respectively. As expected, the VII-L telomere containing only mutant sequence (VII-L-MUT)
102 was longer and more heterogeneous than the wild-type control telomere (VII-L-WT) (Fig.

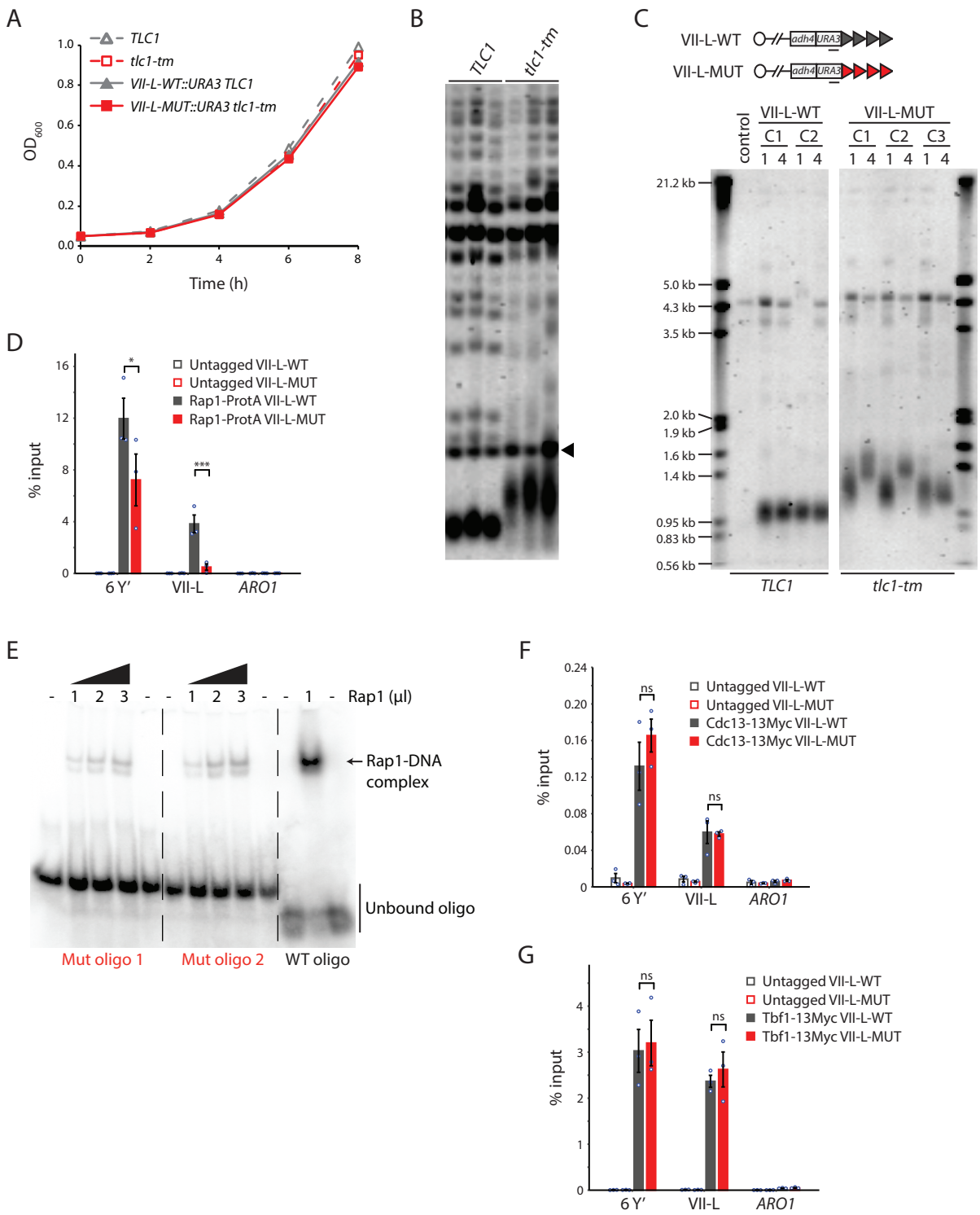

Figure 1. Rap1 binds poorly to *tlc1-tm* telomere sequences

(A) Exponentially growing cells of the indicated genotypes were diluted to an OD_{600} of 0.05 and monitored for 8 h. Three clones of each genotype were followed, and the average of the measurements at each time point is plotted. Error bars are too small to be visualized.

(B) Telomere Southern blot analysis of *TLC1* and *tlc1-tm* cells (three clonal isolates per genotype). Black arrowhead indicates a 1.8 kb DNA fragment generated from the BsmAI-digestion of plasmid pYt103 (Shampay et al., 1984). The major terminal restriction fragment is below the 1.8 kb control band.

(C) Southern blot analysis of the artificial VII-L telomere, with either wild-type or *tlc1-tm* mutant sequence, using a probe to the adjacent *URA3* gene. Multiple clones were examined, with each clone propagated for 1 to 4 passages (each passage corresponds to approximately 25 generations). A wild-type strain (lacking the artificial VII-L telomere) was used as a control.

(D, F, G) ChIP-qPCR analysis of the association of (D) Protein A-tagged Rap1, (F) Myc-tagged Cdc13, and (G) Myc-tagged Tbf1 to six Y' telomeres, the VII-L telomere, or to the non-telomeric *ARO1* locus. Untagged wild-type and *tlc1-tm* strains were used as controls. The mean percentage of input +/- SEM is shown (n=3, ** p<0.01).

(E) EMSA of Rap1 protein incubated with radiolabeled oligonucleotides with either wild-type or tlc1-tm mutant telomeric sequence.

103 1C). We assessed the association of Rap1 to the VII-L-WT or VII-L-MUT telomeres, as well
104 as to native Y′ telomeres, by chromatin immunoprecipitation coupled with quantitative PCR
105 (ChIP-qPCR). Binding of Rap1 is substantially reduced at the VII-L-MUT telomere (Fig.
106 1D). Rap1 is more modestly reduced at Y′ telomeres due to the retention of some wild-type
107 repeats at native telomeres. We confirmed the Rap1 ChIP-qPCR result by performing an
108 electrophoretic mobility shift assay (EMSA) using recombinant full-length Rap1 protein. We
109 find that Rap1 shows a very poor binding capacity to the *tlc1-tm* oligonucleotides compared
110 to the wild-type telomeric sequence (Fig. 1E).

111 Cdc13 is the main sequence-specific single-stranded telomeric DNA binding protein
112 in *S. cerevisiae* (Nugent et al., 1996). Cdc13 requires a minimum of 11 nucleotides of GT-
113 rich sequence for full binding affinity, with only three bases—forming a GNGT motif—
114 recognized with high specificity (Eldridge et al., 2006). The GNGT motif is present in the
115 *tlc1-tm* mutant sequence, so Cdc13 binding should not be altered. Consistent with this
116 hypothesis, we find that Cdc13 associates equally well with both wild-type and mutant
117 telomeres (Fig. 1F).

118 The ability of *tlc1-tm* strains to survive with greatly reduced Rap1 telomere
119 association was surprising given that Rap1 is the main telomere binding protein in *S.*
120 *cerevisiae*, important for recruiting a number of other proteins to telomeres, and is encoded
121 by an essential gene. However, the essential function of Rap1 is likely linked to its ability to
122 bind nontelomeric sites in the genome where it acts as a transcriptional regulator of several
123 hundred genes (Azad & Tomar, 2016). In addition, *S. cerevisiae* strains expressing a mutant
124 telomerase that adds vertebrate TTAGGG telomeric repeats are devoid of Rap1, indicating
125 that Rap1 is not essential for telomere capping (Alexander & Zakian, 2003; Brevet et al.,
126 2003). In these strains, Tbf1 binds to the vertebrate repeats and is able to regulate telomere
127 length homeostasis in a Rap1-independent manner (Alexander & Zakian, 2003; Berthiau et

128 al., 2006). Thus, we assessed binding of Tbf1 to *tlc1-tm* telomeres. We find no change in the
129 levels of Tbf1 at *tlc1-tm* telomeres compared to wild-type telomeres by ChIP-qPCR (Fig.
130 1G), consistent with neither wild-type nor mutant telomere sequences containing the RCCCT
131 Tbf1 consensus binding sequence (Preti et al., 2010), indicating that the loss of Rap1 is not
132 compensated by recruitment of Tbf1. The Tbf1 association observed at the native Y′
133 telomeres is due to the presence of TTAGGG repeats at subtelomeric regions (Brigati et al.,
134 1993), while the association observed at the artificial VII-L telomere is likely due to the
135 presence of several RCCCT motifs in the adjacent sequence (Supplementary Fig. 1).
136
137 **Loss of Rap1-mediated telomere length regulation at *tlc1-tm* telomeres**
138 The decreased binding of Rap1 to *tlc1-tm* sequences likely explains the long, heterogeneous-
139 sized telomeres in *tlc1-tm* strains, because Rap1 negatively regulates telomerase through
140 what is called the "protein counting" model. This model posits that Rap1, through its
141 recruitment of Rif1 and Rif2, inhibits telomerase; the longer a telomere is, the more Rap1,
142 Rif1, and Rif2 will be present, and the stronger the inhibition of telomerase will be (Marcand
143 et al., 1997; Levy & Blackburn, 2004). Reduced binding of Rap1 would cause *tlc1-tm*
144 telomeric sequences to not be recognized as telomeric in terms of Rap1-mediated telomere
145 length regulation. To test this hypothesis, we again modified telomere VII-L to generate a
146 telomere that would be seeded with either 84 bp or 300 bp of *tlc1-tm* telomeric sequence, but
147 in a *TLC1* strain expressing wild-type telomerase so that the tip of the telomere would contain
148 wild-type telomeric sequences. In both cases, the size of the telomere VII-L terminal
149 restriction fragment increased in size, with the magnitude of the increase roughly equivalent
150 to the size of the *tlc1-tm* telomeric seed sequence, indicating that this sequence is not being
151 sensed by the Rap1 protein counting mechanism (Fig. 2A).

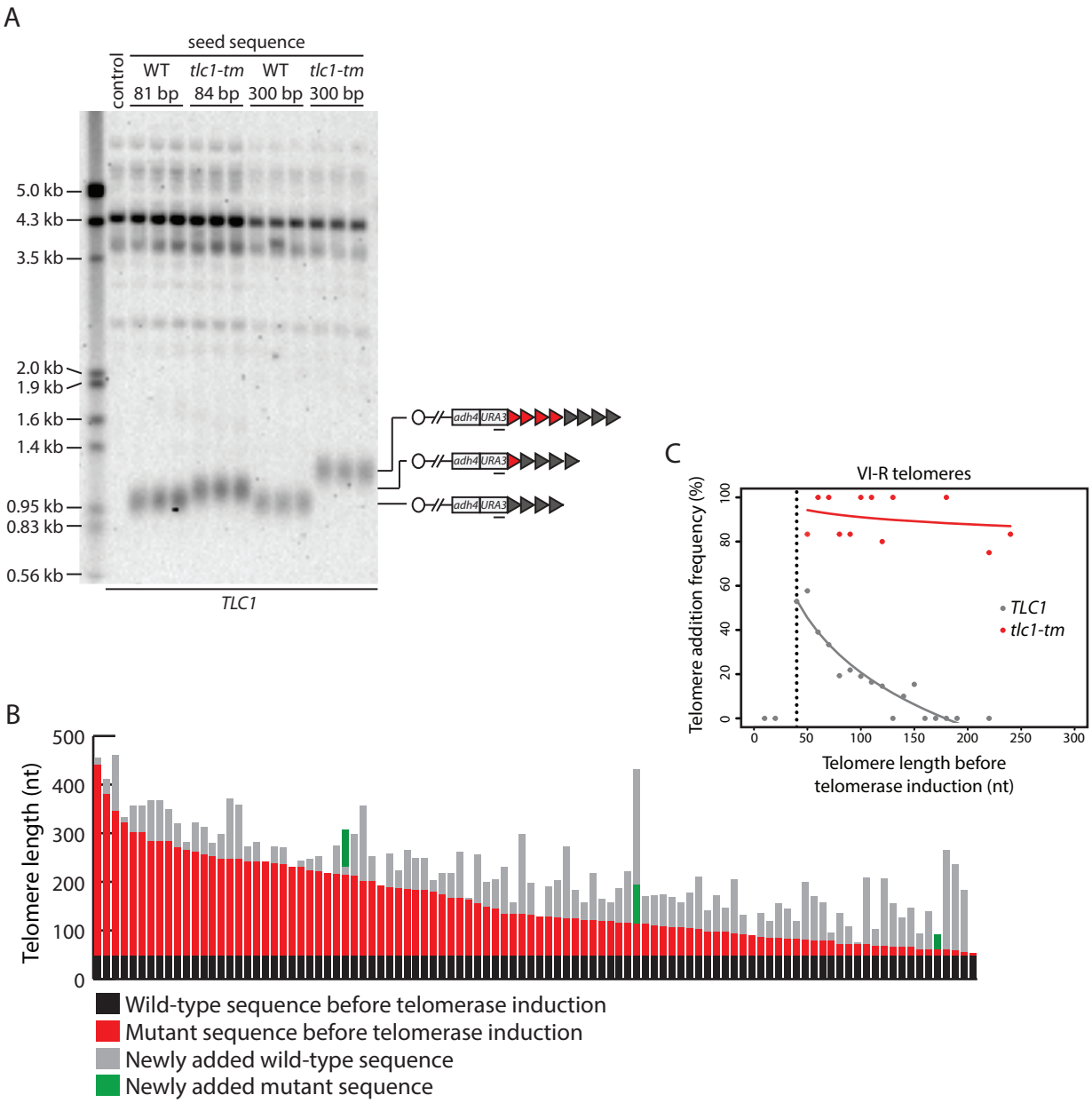

Figure 2. Telomere length regulation is disrupted in *tlc1-tm* cells

(A) Southern blot analysis of the artificial VII-L telomere using a probe to the adjacent *URA3* gene. The telomere was seeded with either wild-type or *tlc1-tm* mutant sequence of the indicated lengths in a strain expressing wild-type *TLC1*. Multiple clones of each strain were examined. A wild-type strain (lacking the artificial VII-L telomere) was used as a control.

(B) In vivo extension of *tlc1-tm* telomeres was examined using the iSTEX assay. Telomere VI-R was amplified and sequenced after the induction of wild-type telomerase. Each bar represents an individual telomere. The black and red portions of each bar represent wild-type and *tlc1-tm* sequence, respectively, that is identical in sequence and thus present before telomerase induction. The length of the black/wild-type sequence is 48 bp. Sequence that is divergent from the black and red sequence is shown in grey and green. Grey represents newly added wild-type sequence after the induction of telomerase. Green represents divergent *tlc1-tm* sequence, most likely a result of homologous recombination. Telomeres are sorted based on the length of the undiverged (black plus red) sequence.

(C) Telomere VI-R sequences obtained from the iSTEX analysis in B were binned into groups of 10 nt in size according to telomere length before telomerase induction. iSTEX data for the extension of wild-type telomeres were taken from previous studies (Strecker et al., 2017; Stinus et al., 2017) and included for comparison. Groups containing less than four telomeres were excluded from this analysis. Frequency of extension and average telomere length before telomerase induction were calculated and plotted for each group. Logarithmic regression curves for each data set were also included in the plot. Telomeres shorter than 40 nt before telomerase induction, which are not efficiently recognized and extended by telomerase (Strecker et al., 2017), were removed from the regression analysis.

152 To examine telomere length regulation in *tlc1-tm* strains further, we monitored
153 telomerase-mediated telomere extension events at nucleotide resolution after a single cell
154 cycle using the iSTEX (inducible Single Telomere EXtension) assay (Strecker et al., 2017).
155 At wild-type telomeres, telomerase extends only a subset of telomeres in each cell cycle, with
156 a strong preference for the extension of short telomeres (Teixeira et al., 2004; Strecker et al.,
157 2017). At *tlc1-tm* telomeres, we find that telomere extension frequency is dramatically
158 increased, with nearly all (92%) of telomeres being extended during a single cell cycle (Fig.
159 2B and 2C). This observation is consistent with the protein counting model; the lack of Rap1
160 at *tlc1-tm* telomeres causes them to all be recognized as short telomeres in need of
161 elongation.
162
163 ***tlc1-tm* telomeres are rapidly degraded in the absence of telomerase**
164 The increase in telomere extension frequency of *tlc1-tm* telomeres is much more dramatic
165 than the increase seen in *rif1*Δ, *rif2*Δ, and *pif1-m2* cells (Teixeira et al., 2004; Stinus et al.,
166 2017), even though these mutants have similar or longer telomeres than the *tlc1-tm* mutant
167 (e.g. see Fig. 5 for comparison to *rif1*Δ and *rif2*Δ). Ablation of Rap1 leads to readily
168 detectable telomere degradation within a few hours (Vodenicharov et al., 2010), so we
169 hypothesized that while decreased Rap1 at *tlc1-tm* telomeres may favor their extension by
170 telomerase, increased degradation may limit the length of *tlc1-tm* telomeres. If true, removal
171 of telomerase should trigger rapid entry into senescence. To test this idea, we sporulated
172 diploid strains that were heterozygous for *EST2*, which encodes the protein catalytic subunit
173 of telomerase (Lingner et al., 1997), or *TLC1*, with either wild-type or mutant telomeres (i.e.
174 *est2Δ/EST2* versus *est2Δ/EST2 tlc1-tm/tlc1-tm* and *tlc1Δ/TLC1* versus *tlc1Δ/tlc1-tm*), and
175 performed senescence assays with the haploid meiotic progeny. In the presence of wild-type
176 telomeres but absence of telomerase (*est2Δ* and *tlc1Δ*), telomeres shortened until the cells

177 senesced after 60 to 70 population doublings, as expected (Fig. 3A). A small subset of the
178 senescent population was then able to lengthen the telomeres by recombination-mediated
179 mechanisms, forming so-called survivors (Lundblad & Blackburn, 1993). We found that cells
180 containing mutant telomeres senesced rapidly, only ~40 population doublings after
181 telomerase loss (Fig. 3A, *est2Δ tlc1-tm** and *tlc1Δ**). We examined the telomere length of
182 cells that had undergone ~30 population doublings after isolation of the haploid spores and
183 found that, upon loss of telomerase, mutant telomeres became extremely heterogeneous and
184 degraded (i.e. a continuous smear of telomeric DNA-hybridizing signal extending from the
185 wells to the bottom; Fig. 3B).
186
187 **Rif1 and Sir4, but not Rif2 nor Sir3, association to *tlc1-tm* telomeres is decreased**
188 Rap1, through its C-terminal domain, recruits Rif1, Rif2, Sir3, and Sir4 to telomeres (Hardy
189 et al., 1992; Wotton & Shore, 1997; Moretti et al., 1994). We reasoned that the reduction of
190 Rap1 at the *tlc1-tm* telomeres should also decrease recruitment of Rif1, Rif2, Sir3, and Sir4,
191 which we tested by ChIP-qPCR (Fig. 4A). Consistent with this hypothesis, we find that Rif1
192 and Sir4 recruitment to the VII-L-MUT telomere is reduced compared to the VII-L-WT
193 telomere (to 16% for Rif1 and 31% for Sir4). Surprisingly, the recruitment of neither Rif2 nor
194 Sir3 is affected. Rif2 can interact with the Xrs2 and Rad50 subunits of the MRX complex
195 (Hirano et al., 2009; Hailemariam et al., 2019; Roisné-Hamelin et al., 2021), which binds to
196 DNA ends and telomeres (Oh & Symington, 2018); Rif2 can also interact directly with
197 double-strand DNA (Cassani et al., 2016; Hailemariam et al., 2019). Sir3 possesses multiple
198 domains that can interact with histones (Gartenberg & Smith, 2016). Thus, Rif2 and Sir3 may
199 associate to *tlc1-tm* telomeres via Rap1-independent mechanisms.
200
201 **Transcription is not affected at *tlc1-tm* telomeres**

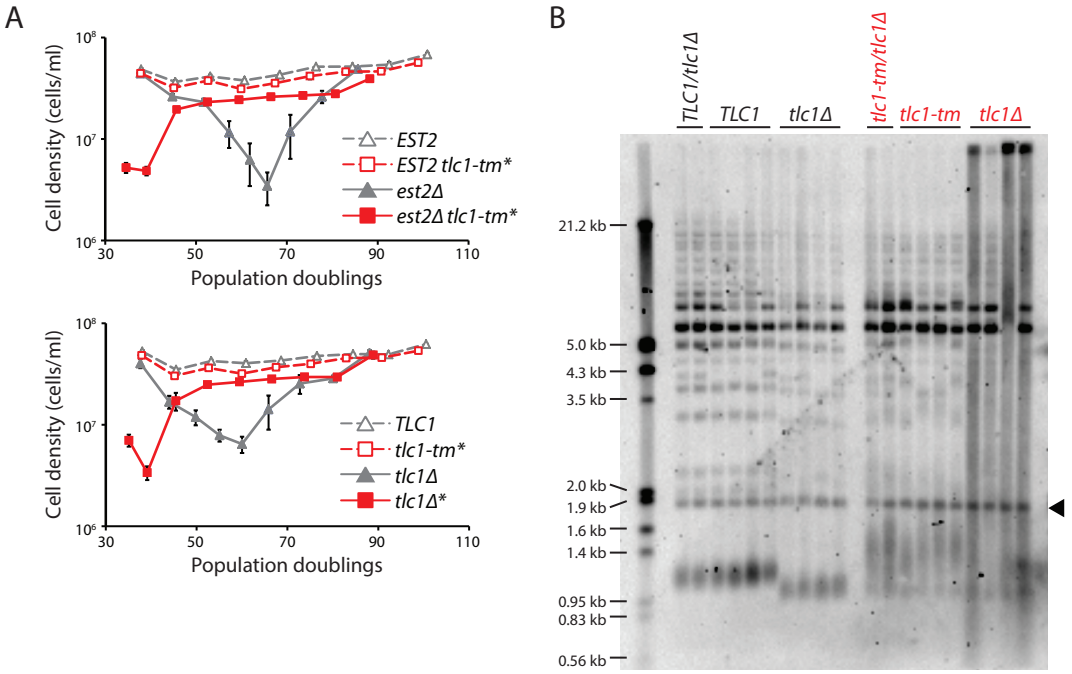

Figure 3. Fast degradation of *tlc1-tm* telomeres in the absence of telomerase

(A) Senescence rates were measured by serial passaging of strains of the indicated genotypes, derived from the sporulation of *est2Δ/EST2* and *est2Δ/EST2 tlc1-tm/tlc1-tm* diploids (top panel) or *tlc1Δ/TLC1* and *tlc1Δ/tlc1-tm* diploids (bottom panel). Cell density was measured every 24 h, followed by dilution to $1x10^5$ cell/ml. Mean +/- SEM of four independent isolates per genotype is plotted.

(B) Telomere Southern blot analysis of samples obtained at the first time point of the senescence assays in A. Black arrowhead indicates the 1.8 kb telomere sequence-containing fragment loaded as control, as in Figure 1B.

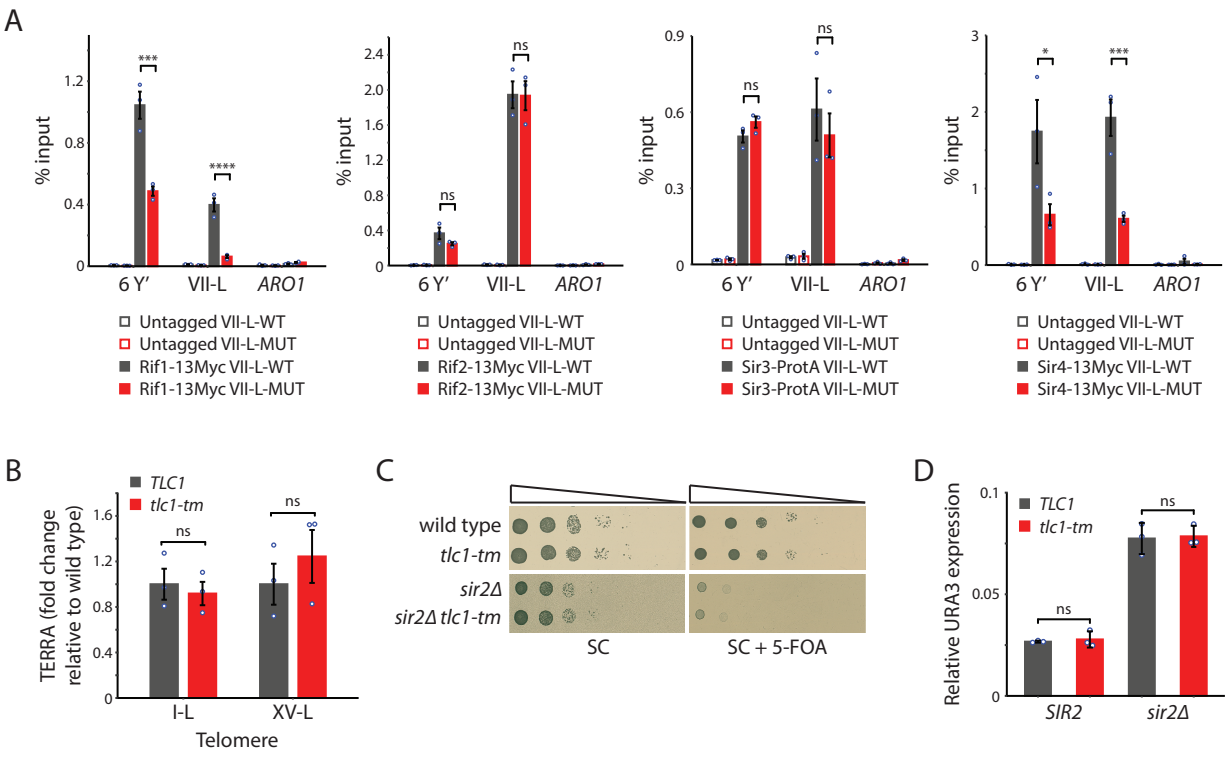

Figure 4. Recruitment of Rif1 and Sir4, but not Rif2 nor Sir3, is significantly reduced at *tlc1-tm* telomeres

(A) ChIP-qPCR analysis of the association of Myc-tagged Rif1, Rif2, Sir4, and Protein A-tagged Sir3 to six Y' telomeres, the VII-L telomere, or to the non-telomeric *ARO1* locus. Untagged wild-type and tlc1-tm strains were used as controls.

(B) Total RNA was reverse transcribed and TERRA from specific telomeres (I-L and XV-L) was analyzed by qPCR. TERRA values were normalized to ACT1 levels, and to the respective wild type (*TLC1*).

(C) Tenfold serial dilutions of strains with the indicated genotypes were spotted on SC plates without or with 5-FOA.

(D) The expression of the subtelomerically integrated *URA3* gene was measured in the indicated yeast strains by RT-qPCR.

All data (except C) are shown as mean +/- SEM (n=3, *** $p<10^{-3}$, **** $p<10^{-4}$).

202 Rap1, through its recruitment of the Rif and Sir proteins, represses the transcription of non-
203 coding telomeric repeat-containing RNA (TERRA) (Iglesias et al., 2011). Reduced levels of
204 Rap1, Rif1, and Sir4 at *tlc1-tm* telomeres may alter TERRA transcription. However, we find
205 no change in TERRA abundance in *tlc1-tm* cells (Fig. 4B). Rap1, through its recruitment of
206 the Sir complex, also mediates the transcriptional silencing of subtelomeric genes (Moretti et
207 al., 1994). The VII-L-WT and VII-L-MUT telomeres possess a *URA3* gene immediately
208 adjacent to the telomeric repeats. Silencing of the *URA3* gene was monitored by assaying for
209 growth in the presence of 5-fluoroorotic acid (5-FOA), which kills cells expressing *URA3*
210 (Fig. 4C). Strains deleted for *SIR2*, which causes a defect in silencing (Aparicio et al., 1991),
211 were used as controls. Because hypersensitivity to 5-FOA does not correlate with loss of
212 silencing in some genetic backgrounds (Rossmann et al., 2011), we also measured URA3
213 transcript levels by reverse-transcriptase quantitative PCR (Fig. 4D). In both assays, we find
214 no difference between VII-L-WT and VII-L-MUT, indicating that the reduced levels of Rap1
215 and Sir4 at *tlc1-tm* telomeres still allow functional silencing.
216
217 **Rif2 prevents degradation of *tlc1-tm* telomeres**
218 Rap1 regulates telomere length homeostasis through its recruitment of Rif1, Rif2, and Sir4.
219 Rif1 and Rif2 negatively regulate telomerase (Hardy et al., 1992; Wotton & Shore, 1997;
220 Levy & Blackburn, 2004). In contrast, Sir4 functions in a pathway to recruit telomerase to
221 telomeres (Hass & Zappulla, 2015). We tested what effect deleting *RIF1*, *RIF2*, and *SIR4*
222 would have on telomere length in *tlc1-tm* cells. Deletion of *SIR4* results in a small decrease in
223 telomere length in *TLC1* cells, as expected (Hass & Zappulla, 2015), but no noticeable
224 change in *tlc1-tm* cells (Fig. 5A). The lack of an effect could be due to Sir4 already being
225 reduced at *tlc1-tm* telomeres (Fig. 4A). Deletion of *RIF1* increases telomere length in both
226 *TLC1* and *tlc1-tm* cells (Fig. 5B and Supplementary Fig. 2), despite Rif1 also being reduced

227 at *tlc1-tm* telomeres (Fig. 4A). Rif1 may still impact *tlc1-tm* telomeres because it plays a
228 much bigger role in telomere length homeostasis than Sir4.
229 Deletion of *RIF2* causes dramatic degradation of *tlc1-tm* telomeres, with a continuous
230 smear of telomeric DNA-hybridizing signal observed (Fig. 5B and Supplementary Fig. 2),
231 similar to *tlc1-tm* cells upon loss of telomerase (Fig. 3B). This finding, along with the
232 observation that Rif2 is still present at *tlc1-tm* telomeres (Fig. 4A), indicates that Rif2 has an
233 important role in protecting *tlc1-tm* telomeres. Since uncapped telomeres expose
234 chromosome ends to non-homologous end joining (NHEJ) and homologous recombination
235 (HR), we tested whether the *rif2*Δ *tlc1-tm* telomere profile would change by deleting *DNL4*
236 or *RAD52*, which are required for NHEJ and HR, respectively (Wilson et al., 1997;
237 Symington et al., 2014). The extensive smear was still observed in *dnl4*Δ *rif2*Δ *tlc1-tm* and
238 *rad52*Δ *rif2*Δ *tlc1-tm* triple mutants, but was reduced in intensity, especially at low molecular
239 weight, in *rad52*Δ *rif2*Δ *tlc1-tm* (Fig. 5C). *rif2*Δ *tlc1-tm* cells grow poorly, and this growth
240 defect is exacerbated by additional deletion of *RAD52*; *rad52*Δ *rif2*Δ *tlc1-tm* spores mostly
241 fail to germinate, and those that do grow even more poorly than *rif2*Δ *tlc1-tm* (Fig. 5D-E),
242 suggesting that Rad52-mediated HR helps cope with *rif2*Δ *tlc1-tm* uncapped telomeres.
243 Interestingly, *rif1*Δ *rif2*Δ and *rif1*Δ *rif2*Δ *tlc1-tm* cells have very similar telomere
244 profiles: very long telomeres but without the extensive degradation seen in *rif2*Δ *tlc1-tm* cells
245 (Fig. 5B). This observation is reminiscent of the elevated levels of telomere-telomere fusion
246 seen in *rif2*Δ *tel1*Δ cells, and not in *rif1*Δ *rif2*Δ *tel1*Δ cells (Marcand et al., 2008), but it is
247 currently unclear whether there is a common underlying mechanism that explains both
248 observations.
249
250 **Rif2 protects *tlc1-tm* telomeres by inhibiting the MRX complex**

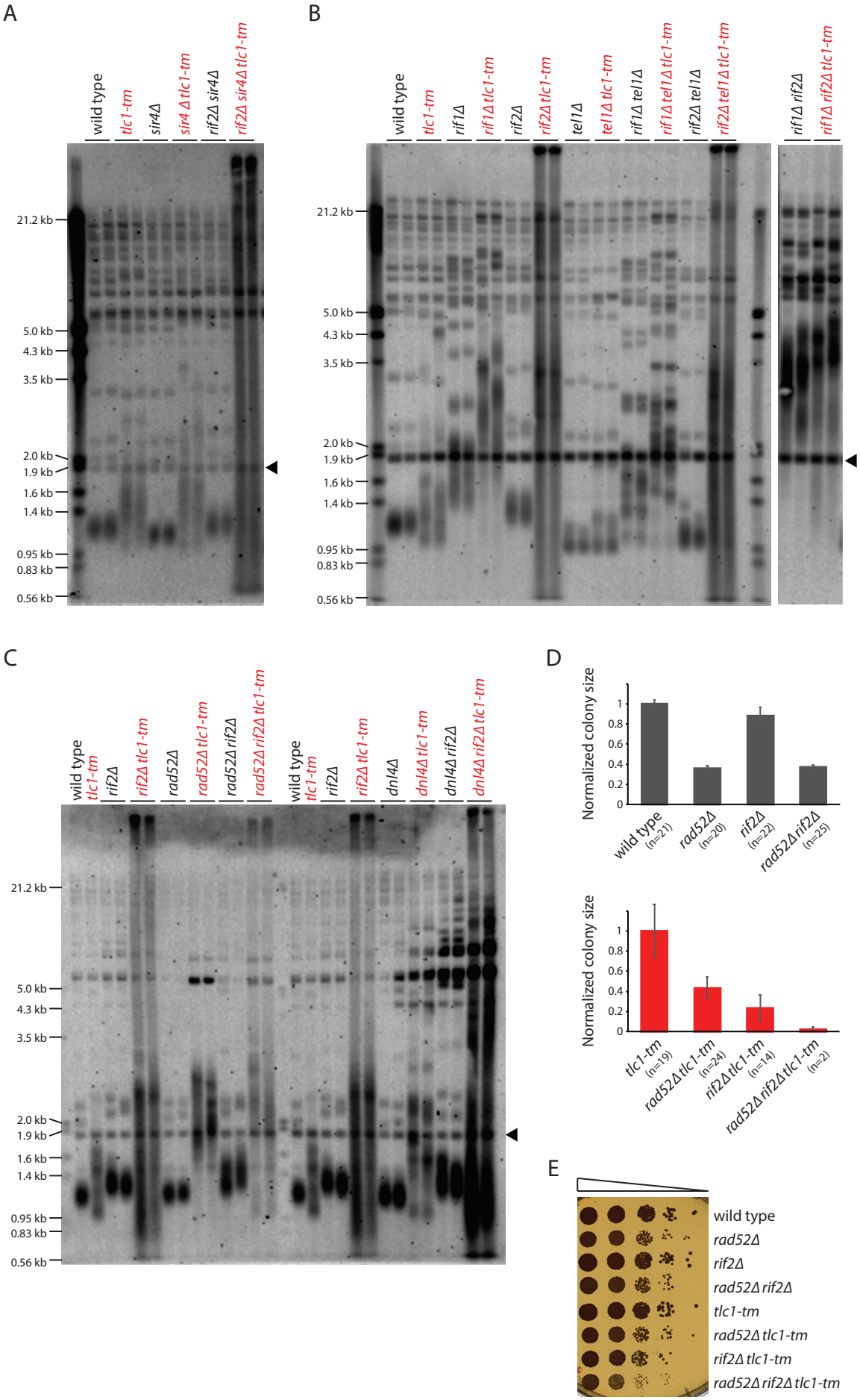

Figure 5. Rif2 prevents degradation of *tlc1-tm* telomeres

(A-C) Telomere Southern blot analysis of strains of the indicated genotypes. Black arrowhead indicates the 1.8 kb telomere sequence-containing fragment loaded as control, as in Figure 1B.

(D) Colony sizes of haploid meiotic progeny derived from the sporulation of *rad52Δ/RAD52 rif2Δ/RIF2* and *rad52Δ/RAD52 rif2Δ/RIF2 tlc1-tm/tlc1-tm* diploid strains were measured and normalized to wild-type (top panel) or *tlc1-tm* (bottom panel). The number of colonies analyzed is indicated in parenthesis. Error bars show SEM.

(E) Tenfold serial dilutions of strains with the indicated genotypes were spotted on YPD plates and grown at 30ºC.

251 *TEL1* is epistatic to *RIF2* with respect to telomere length regulation; while *rif2*Δ cells have
252 long telomeres, *tel1*Δ and *rif2*Δ *tel1*Δ cells have very short telomeres (Craven & Petes, 1999).
253 Thus, we tested whether the same would be true in terms of the telomere degradation seen in
254 *rif2*Δ *tlc1-tm* cells. Deletion of *TEL1* shortens the telomeres of *tlc1-tm* cells, but does not
255 affect the telomere profile of *rif2*Δ *tlc1-tm* cells (Fig. 5B), indicating that Rif2 does not
256 inhibit Tel1 to prevent the degradation of *tlc1-tm* telomeres. Recent studies have shown that
257 Rif2 attenuates Tel1 activity at telomeres by inhibiting the MRX complex (consisting of
258 Mre11, Rad50, and Xrs2), which is responsible for recruiting Tel1 to telomeres (Hailemariam
259 et al., 2019; Sabourin et al., 2007). Rif2 discharges the ATP-bound state of Rad50, thereby
260 making the MRX complex incapable of activating Tel1 (Hailemariam et al., 2019). Similarly,
261 Rif2 enhancement of Rad50 ATPase activity limits MRX-mediated tethering of DNA ends
262 during double-strand break repair (Cassani et al., 2016). Rif2 also inhibits MRX-mediated
263 resection of telomeric DNA ends (Bonetti et al., 2010a; Bonetti et al., 2010b). Rif2 inhibition
264 of the MRX complex involves a direct interaction between the BAT/MIN motif of Rif2 with
265 the ATPase domain of Rad50 (Roisné-Hamelin et al., 2021; Khayat et al., 2021). Therefore,
266 we hypothesized that Rif2 could be inhibiting MRX-mediated degradation of *tlc1-tm*
267 telomeres. Consistent with this idea, we find that Mre11 is about fivefold more associated
268 with the VII-L-MUT telomere in comparison with the VII-L-WT telomere (Fig. 6A), and that
269 the telomere degradation observed in *rif2*Δ *tlc1-tm* cells is absent in *rad50*Δ *rif2*Δ *tlc1-tm*
270 cells (Fig. 6B).
271 The *rad50*Δ *tlc1-tm* and *rad50*Δ *rif2*Δ *tlc1-tm* cells (also *cdc13-1 tlc1-tm* cells,
272 discussed below) show a telomere profile reminiscent of type II survivors, which maintain
273 their telomeres in a telomerase-independent manner that relies on recombination-mediated
274 amplification of telomeric sequence (Lundblad & Blackburn, 1993; Teng & Zakian, 1999).
275 Independently generated isogenic isolates of type II survivors will have similar but slightly

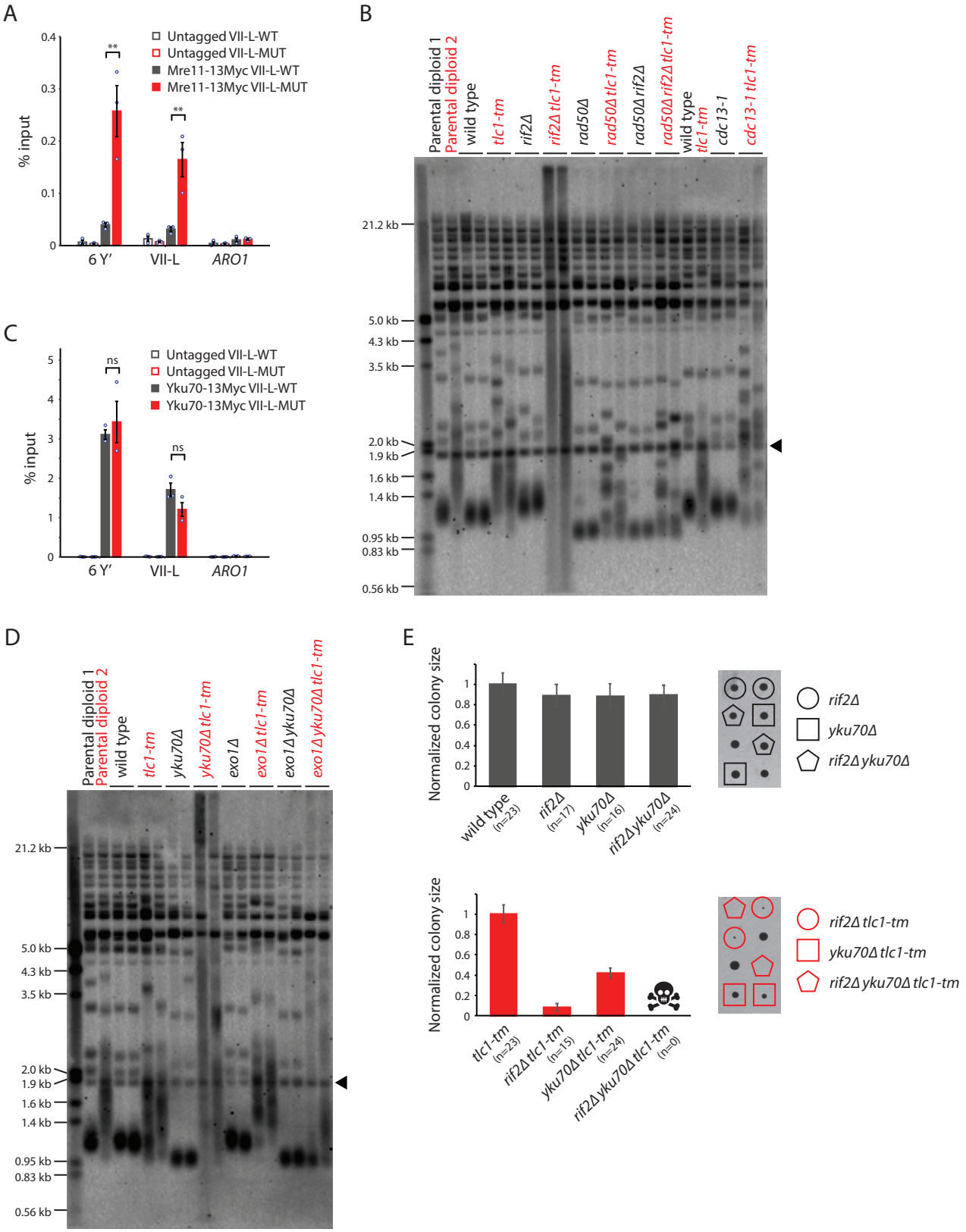

Figure 6. Rif2 protects *tlc1-tm* telomeres by inhibiting the MRX complex and acts in parallel with the Yku complex
(A&C) ChIP-qPCR analysis of the association of Myc-tagged Mre11 and Yku70 to six Y' telomeres, the VII-L telomere, or to the non-telomeric *ARO1* locus. Untagged wild-type and *tlc1-tm* strains were used as controls. The mean percentage of input +/- SEM is shown (n=3, ** p<0.01).
(B&D) Telomere Southern blot analysis of strains of the indicated genotypes. Black arrowhead indicates the 1.8 kb telomere sequence-containing fragment loaded as control, as in Figure 1B. (B) Parental diploid 1 is *rad50Δ/RAD50 rif2Δ/RIF2*; parental diploid 2 is *rad50Δ/RAD50 rif2Δ/RIF2 tlc1-tm/tlc1-tm*. The last six lanes are derived from cells grown at 22°C. (D) Parental diploid 1 is *exo1Δ/EXO1 yku70Δ/YKU70*; parental diploid 2 is *exo1Δ/EXO1 yku70Δ/YKU70 tlc1-tm/tlc1-tm*.
(E) Colony sizes of haploid meiotic progeny derived from the sporulation of *rif2Δ/RIF2 yku70Δ/YKU70* and *rif2Δ/RIF2 yku70Δ/YKU70 tlc1-tm/tlc1-tm* diploid strains were measured and normalized to wild-type (top panel) or *tlc1-tm* (bottom panel). The number of colonies analyzed is indicated in parenthesis. Error bars show SEM. Representative images of dissected tetrads are shown on the right. Each column of colonies arose from a single tetrad.

276 different telomere profiles, much like that observed in different isolates of isogenic *tlc1-tm*
277 strains (as seen in *rad50*Δ *tlc1-tm* and *rad50*Δ *rif2*Δ *tlc1-tm* cells, but also in *tlc1-tm* strains in
278 general). However, this effect is still observed in *rad50*Δ *tlc1-tm* and *rad50*Δ *rif2*Δ *tlc1-tm*
279 strains with an additional deletion of *RAD52*, which is required for homologous
280 recombination and survivor formation (Lundblad & Blackburn, 1993; Claussin & Chang,
281 2015) (Supplementary Fig. 3A). Interestingly, the severe growth defect of *rad52*Δ *rif2*Δ *tlc1-*
282 *tm* strains (Fig. 5D) is suppressed by an additional deletion of *RAD50* (Supplementary Fig.
283 3B). At present, we do not know the reason for the slight telomere profile differences seen
284 between different isolates of isogenic *tlc1-tm* strains, but it may be related to a previous
285 observation that the very tip of the telomere has unique sequence features that affect telomere
286 capping and length regulation (Grossi et al., 2001).
287
288 **Rif2 and the Yku complex act in parallel to protect *tlc1-tm* telomeres**
289 The CST (Cdc13-Stn1-Ten1) and Yku (Yku70-Yku80) complexes are also important for
290 inhibiting nucleolytic degradation at telomeres (Garvik et al., 1995; Grandin et al., 1997;
291 Grandin et al., 2001; Gravel et al., 1998), and their importance might be increased at *tlc1-tm*
292 telomeres. Cdc13 and Yku70 are present at similar levels at VII-L-WT and VII-L-MUT
293 telomeres (Fig. 1F; Fig. 6C). The *cdc13-1* temperature-sensitive mutant causes an
294 accumulation of single-stranded telomeric DNA (Garvik et al., 1995), and is defective even at
295 the permissive temperature of 23°C (Paschini et al., 2012). *cdc13-1 tlc1-tm* cells do not
296 exhibit the extensive telomere degradation seen in *rif2*Δ *tlc1-tm* cells (Fig. 6B). In contrast,
297 we observe extensive telomere degradation in *yku70*Δ *tlc1-tm* cells (Fig. 6D). Telomere
298 degradation is not seen in *exo1*Δ *yku70*Δ *tlc1-tm* cells, suggesting that the Yku complex
299 inhibits the Exo1 exonuclease to protect *tlc1-tm* telomeres. *rif2*Δ *yku70*Δ *tlc1-tm* cells are not

300 viable (Fig. 6E), indicating that Rif2 and the Yku complex function in parallel to protect *tlc1-*
301 *tm* telomeres.
302
303 **Rif2 recruitment to *tlc1-tm* telomeres requires a DNA end and the MRX complex**
304 The telomere degradation seen in *tlc1-tm rif2*Δ cells has also been observed in other *tlc1*
305 template mutants, such as the *tlc1-476A* mutant (Fig. 7A), even without deletion of *RIF2*
306 (Chan et al., 2001; Lin et al., 2004). The *tlc1-476A* mutant changes the invariable CCC core
307 of the template region to CAC, causing the addition of long stretches of TG dinucleotide
308 repeats, occasionally interrupted by a TGG trinucleotide, that are predicted to disrupt Rap1
309 binding even more so than *tlc1-tm* repeats (Chan et al., 2001; Graham & Chambers, 1994).
310 We find that *tlc1-476A* mutants are completely dependent on Rif2 for survival, as *tlc1-476A*
311 *rif2*Δ double mutants are inviable (Fig. 7B).
312 To examine how Rif2 is able to associate with the Rap1-depleted telomeres of *tlc1-tm*
313 cells, we first asked whether a DNA end is required. We inserted 300 bp of either wild-type
314 or *tlc1-tm* telomeric sequence at an internal genomic locus on chromosome III (III-ITS;
315 chromosome III interstitial telomeric sequence) and assessed Rif2 association by ChIP-qPCR.
316 We find that Rif2 associates with the wild-type ITS, but not the *tlc1-tm* ITS (Fig. 7C),
317 indicating that Rap1-independent recruitment of Rif2 to *tlc1-tm* sequence requires a DNA
318 end. Since the MRX complex binds to DNA ends and telomeres (Oh & Symington, 2018),
319 and Rif2 is known to interact with both Rad50 and Xrs2 (Hirano et al., 2009; Hailemariam et
320 al., 2019; Roisné-Hamelin et al., 2021), Rif2 recruitment to *tlc1-tm* telomeres might require
321 the MRX complex. Consistent with this hypothesis, we find that Rif2 association to the *tlc1-*
322 *tm* telomeres is lost in *rad50*Δ strains (Fig. 7D).
323
324 **Discussion**

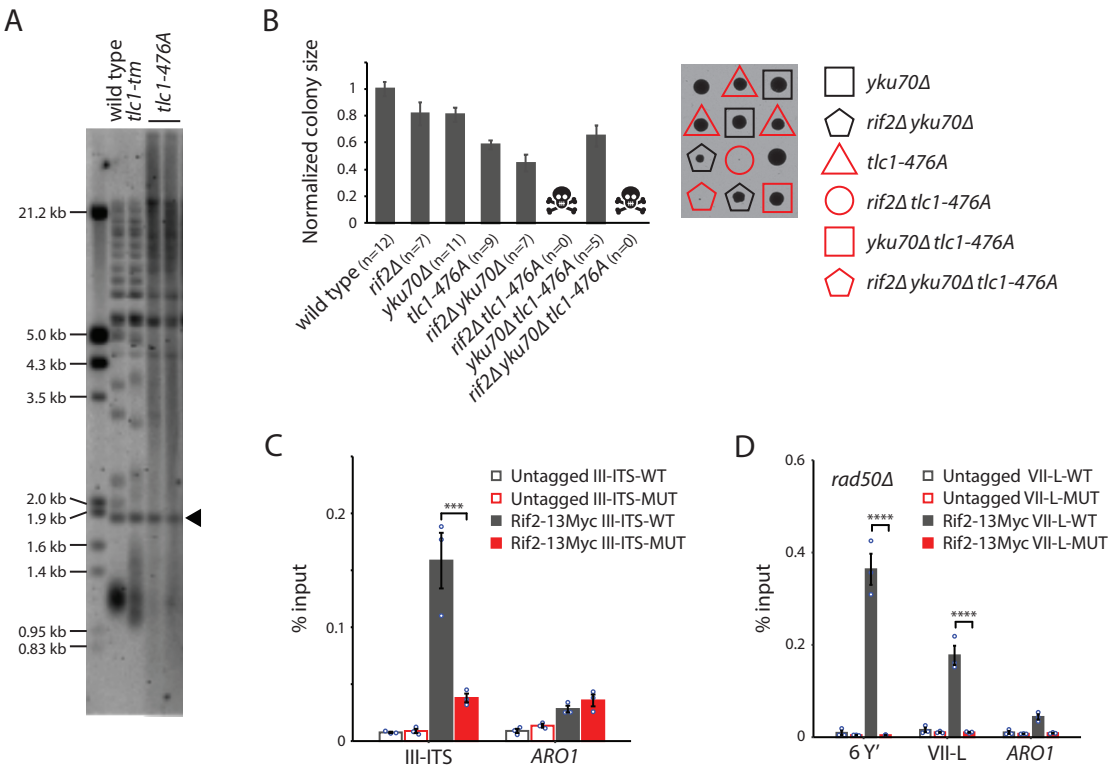

Figure 7. Rif2 association to *tlc1-tm* telomeres requires the MRX complex

(A) Telomere Southern blot analysis of strains of the indicated genotypes. Black arrowhead indicates the 1.8 kb telomere sequence-containing fragment loaded as control, as in Figure 1B.

(B) Colony sizes of haploid meiotic progeny derived from the sporulation of a *rif2Δ/RIF2 yku70Δ/YKU70 tlc1-476A/TLC1* diploid strain were measured and normalized to wild-type. The number of colonies analyzed is indicated in parenthesis. Error bars show SEM. Representative images of dissected tetrads are shown on the right. Each column of colonies arose from a single tetrad.

(C) ChIP-qPCR analysis of the association of Myc-tagged Rif2 to a 300-bp ITS located on chromosome III containing either wild-type or *tlc1-tm* sequence. The mean percentage of input +/- SEM is shown (n=3, *** $p<10^{-3}$).

(D) ChIP-qPCR analysis of the association of Myc-tagged Rif2 to six Y' telomeres, the VII-L telomere, or to the non-telomeric *ARO1* locus in a *rad50Δ* background. Untagged strains were used as controls. The mean percentage of input +/- SEM is shown (n=3, **** $p<10^{-4}$).

325 In this study, we investigated the consequences of depleting Rap1 from *S. cerevisiae*
326 telomeres. Our findings suggest that impairing Rap1 binding does not significantly affect cell
327 proliferation. The depletion of telomeric Rap1 causes defects in telomere length regulation
328 and telomere capping. Surprisingly, Rif2 is still recruited to Rap1-depleted telomeres, and its
329 recruitment is dependent on the MRX complex. *tlc1-tm* telomeres become extensively
330 degraded in the absence of Rif2 or the Yku complex, and *rif2*Δ *yku70*Δ *tlc1-tm* triple mutants
331 are inviable. Thus, Rap1, Rif2, and the Yku complex perform separate tasks at telomeres that
332 are together essential for telomere capping and cell viability.

333 Telomere capping is essential for cell viability; yeast cells cannot survive the loss of a
334 single telomere (Sandell & Zakian, 1993). Telomere capping is executed by telomere-binding
335 proteins, so it was surprising to find that yeast cells can survive when Rap1, the main protein
336 that binds double-stranded telomeric DNA, is significantly reduced at telomeres. Previous
337 studies have reported that telomeres of *S. cerevisiae* expressing mutant telomerase that adds
338 TTAGGG repeats are also devoid of Rap1; however, the absence of Rap1 in this situation
339 appears to be compensated by the binding of Tbf1 to the TTAGGG sequence (Alexander &
340 Zakian, 2003; Brevet et al., 2003; Berthiau et al., 2006). In contrast, there is no change in
341 Tbf1 binding at *tlc1-tm* telomeres (Fig. 1G). The difference between yeast telomeres with
342 TTAGGG repeats and *tlc1-tm* telomeres is further highlighted by the fact that Rif2 is absent
343 at the former (Alexander & Zakian, 2003), but is crucial for telomere protection of the latter.
344 In addition, multiple viable *tlc1* template mutants, including *tlc1-tm*, result in the addition of
345 mutant telomeric sequence that does not conform to the consensus binding sites of both Rap1
346 and Tbf1 (Prescott & Blackburn, 2000; Förstemann et al., 2003; Lin et al., 2004), supporting
347 the notion that telomeres can remain sufficiently capped in the absence of both proteins.

348 Previously studied *tlc1* template mutations that abolish Rap1 binding to the resulting
349 mutant telomere sequences generally fall into two categories; they either cause telomere

350 shortening or they cause rapid telomere elongation, which in some cases is accompanied by
351 extensive telomere degradation (Prescott & Blackburn, 2000; Lin et al., 2004), similar to that
352 seen in *rif2*Δ *tlc1-tm* mutants (Fig. 5B). The first category is likely due to a loss of telomerase
353 enzymatic activity, because most *tlc1* template mutations result in a reduction in the
354 nucleotide addition processivity of telomerase (Förstemann et al., 2003). The extent of
355 telomere elongation and degradation in the second category appears to be correlated with the
356 decrease in Rap1 binding (Prescott & Blackburn, 2000). Rap1 association to fully mutant
357 *tlc1-tm* telomeres is reduced to approximately 13% compared to wild-type telomeres (Fig.
358 1D). We suspect that this level of Rap1 prevents the more extensive elongation and
359 degradation seen in several other *tlc1* template mutants (e.g. *tlc1-476A*; Fig. 7A) that likely
360 have even less Rap1 telomere association (Prescott & Blackburn, 2000; Lin et al., 2004).
361 Consistent with this hypothesis, *tlc1*Δ cells derived from the sporulation of *tlc1-tm/tlc1*Δ
362 diploids with mutant telomeres also exhibit extensive degradation (Fig. 3B), which is likely
363 the result of further reducing Rap1 telomere association due to telomere shortening.
364 Our findings build upon previous work to show that Rap1 and Rif2 inhibit the MRX
365 complex to prevent telomere degradation. First, decreased telomere association of Rap1 in
366 *tlc1-tm* cells (Fig. 1D) is accompanied by an increase in Mre11 telomere association (Fig.
367 6A), which is consistent with a previous report showing that Rap1 binding inhibits Mre11
368 recruitment (Negrini et al., 2007). Second, the telomere degradation observed in *rif2*Δ *tlc1-tm*
369 cells is eliminated by deletion of *RAD50* (Fig. 6B), which is consistent with previous studies
370 showing that Rif2 inhibits the MRX complex by discharging the ATP-bound form of Rad50
371 (Cassani et al., 2016; Hailemariam et al., 2019). Rif2 and the Yku complex have previously
372 been shown to separately inhibit the resection of telomeric ends in *TLC1* cells, but *rif2*Δ *yku*Δ
373 double mutants remain viable (Bonetti et al., 2010a; Bonetti et al., 2010b). In contrast, we
374 find that *rif2*Δ *yku70*Δ *tlc1-tm* cells are inviable (Fig. 6E), indicating that Rap1 has an

375 important role alongside Rif2 and the Yku complex to inhibit telomere degradation.
376 Furthermore, the inviability of *tlc1-476A rif2*Δ double mutants (Fig. 7B) indicates that Rap1
377 and Rif2 are more important than the Yku complex in this regard.
378 The redundant capping mechanisms offer an explanation for the rapid evolution of the
379 telomere sequence and telomere binding proteins in budding yeast species of the
380 Saccharomycotina subdivision, of which *S. cerevisiae* is a member (Steinberg-Neifach &
381 Lue, 2015). Alterations in the template region of telomerase RNA or in the DNA binding
382 domain of telomere-binding proteins are more easily tolerated if there are redundant
383 mechanisms to ensure sufficient telomere capping and, therefore, cell viability. Indeed, the
384 budding yeast *Kluyveromyces lactis* can also tolerate changes to the template region of its
385 telomerase RNA that disrupts binding to Rap1 (Krauskopf & Blackburn, 1996). The more
386 distantly related fission yeast *Schizosaccharomyces pombe* can also survive without its main
387 telomere-binding protein, Taz1 (Cooper et al., 1997), suggesting that redundancy of telomere
388 capping mechanisms has also evolved independently outside of the Saccharomycotina
389 subdivision.
390 The association of Rif2 to Rap1-depleted *tlc1-tm* telomeres was unexpected given the
391 well-characterized role of the Rap1 C-terminal domain in recruiting Rif2 to telomeres
392 (Wotton & Shore, 1997; Shi et al., 2013). We find that this Rap1-independent recruitment of
393 Rif2 is dependent on the MRX complex (Fig. 7D), which itself is increased at *tlc1-tm*
394 telomeres (as determined by ChIP-qPCR analysis of Mre11; Fig. 6A). The MRX complex
395 plays a central role in the repair of double-strand breaks (DSBs) (Oh & Symington, 2018), so
396 why does Rif2 play such a negligible role? It has recently been reported that Rif2 and Sae2
397 have opposing roles in regulating the MRX complex, and the role of Rif2 in DSB repair is
398 more readily detected in the absence of Sae2 (Marsella et al., 2021). While Sae2 has a
399 prominent role in DSB repair, it has a minor role at telomeres (Bonetti et al., 2009); the

400 inverse is true of Rif2 at DSBs and telomeres. Thus, Sae2 appears to limit Rif2 function at
401 DSBs, and Rif2 may limit the role of Sae2 at telomeres. In wild-type cells, the prominent role
402 of Rif2 at telomeres can be explained by its recruitment by Rap1. However, it is unclear how
403 Rif2 maintains its prominent role at telomeres without Rap1-dependent recruitment. One
404 possibility is that there is preferential recruitment of Sae2 to DSBs compared to telomeres.
405 Further studies are needed to examine this hypothesis.
406

407 ## Materials and Methods

408 **Yeast strains and plasmids**

409 Standard yeast media and growth conditions were used (Sherman, 2002; Lundblad & Struhl,
410 2010). Yeast strains used in this study are listed in Supplementary Table S1. The artificial
411 VII-L telomere was created essentially as previously described (Gottschling et al., 1990), by
412 transforming restriction-digested pVII-L URA-TEL plasmid into yeast. To obtain different
413 versions of the VII-L telomere, this plasmid was modified by replacing the original 81 bp of
414 telomeric repeats with oligonucleotides containing wild-type or *tlc1-tm* telomeric sequence of
415 different length (Supplementary Table S2). Myc and protA C-terminal epitope-tagged
416 proteins were created by integrative transformation of 13 copies of the human c-myc (Myc)
417 epitope or the Staphylococcal protein A IgG binding domain.
418

419 **Southern blotting**

420 Southern blots to detect native telomeres were performed essentially as previously described
421 (van Mourik et al., 2018). Yeast genomic DNA was isolated using a Wizard Genomic DNA
422 Purification Kit (Promega) and digested with XhoI. For each sample, 4 µg of digested
423 genomic DNA, along with 1.25 ng of BsmAI-digested pYt103 (Askree et al., 2004), was
424 separated on a 0.8% (w/v) agarose gel, and transferred to a Hybond-N+ membrane (GE

425 Healthcare). The membrane was hybridized to telomere-specific digoxygenin-labeled probe
426 (wild type probe: 5′-CACCACACCCACACACCACACCCACA-3′; *tlc1-tm* mutant probe:
427 5′-ACCACACCACACCACACACACCACAC-3′). For detection of the artificial VII-L
428 telomere, a similar procedure was performed, except that 6 µg yeast genomic DNA was
429 digested with EcoRV and the membrane was hybridized at 42ºC with a digoxigenin-labeled
430 probe complementary to *URA3* sequence. Unless otherwise mentioned (i.e. Fig. 1C and 3B),
431 all strains were propagated for at least 100 generations before Southern blot analysis.
432
433 **Chromatin immunoprecipitation and quantitative PCR (ChIP-qPCR)**
434 ChIP-qPCR was performed essentially as previously described (Graf et al., 2017). For protein
435 A ChIP, IgG Sepharose 6 Fast Flow beads (GE Healthcare) were used. For Myc ChIP,
436 nProtein A Sepharose 4 Fast Flow beads (GE Healthcare) were used; after preclearing, 9 µl
437 anti-c-Myc Monoclonal antibody (Clontech/Takara) were added to each sample. qPCR was
438 performed using a LightCycler 480 II (Roche) and SYBR-Green (Thermo Scientific)
439 detection with an annealing temperature of 60ºC (40 cycles). Primers are listed in
440 Supplementary Table S3. Measured Cq values were corrected to input and graphs were
441 created using R. All strains were propagated for ~50 generations before ChIP-qPCR analysis.
442
443 **Electrophoretic mobility shift assay (EMSA)**
444 The recombinant *S. cerevisiae* Rap1 full-length protein was expressed in *E. coli* BL21 cells
445 as previously described (Wahlin & Cohn, 2000). The ability of Rap1 to bind the *tlc1-tm*
446 telomeric sequences was assessed by EMSA with two double-stranded (ds) oligonucleotides
447 containing representative sequences; Mut-1 5'-
448 *GTCATACGTCACAC*TGTGGTGTGTGGTGTGGTGTGTGGTGGTGGTGTGTGT-3' (37
449 bp) and Mut-2 5'-

450 *GTCATACGTCACAC*TGTGGTGTGTGTGGTGTGTGGATTTGGTGTGTGG-3' (34 bp).
451 The respective G-rich forward strands and C-rich reverse strands were annealed in 1 mM
452 Tris-HCl, pH 8.0, 0.1 mM $MgCl_2$ by boiling for 2 min and slowly cooling down to room
453 temperature. The correct annealing was guided by the 14 nt non-telomeric region indicated in
454 italics. A ds-oligonucleotide with wild-type telomeric sequence was used as the positive
455 binding control: 5'-TGTGGTGTGTGGGTGTGTG-3' (19 bp). The 5' ends of ds-probes were
456 radioactively labelled with [γ-^{32}P]-ATP using T4 polynucleotide kinase (New England
457 Biolabs), purified on Illustra Microspin G-25 columns (GE), and diluted in 10 mM Tris-HCl,
458 pH 7.5. In binding assays, 10 fmol of labelled probe was mixed with 1.5 µg competitor mix
459 (0.5 µg each of sheared *E.coli* DNA (~250 bp), salmon sperm DNA, and yeast t-RNA) in 1x
460 Binding buffer (10 mM Tris-HCl, pH 7.5, 7 mM $MgCl_2$, 8% glycerol), and varying amounts
461 (~0.1-0.4 µg) of Rap1 protein extract, in a total of 15 µl. The binding reaction was incubated
462 at 25°C for 15 min and then loaded onto 4% polyacrylamide gels (29:1 acrylamide:bis-
463 acrylamide) and run in 1x TBE (89 mM Tris-borate, 2 mM EDTA, pH 8.0), 150V at 4°C.
464 Radioactive signals from dried gels were visualized with a Typhoon FLA 9500 biomolecular
465 imager (GE Life Sciences).
466
467 **Inducible STEX (iSTEX) assay**
468 iSTEX was performed essentially as previously described (Strecker et al., 2017), except that
469 the starting P_{GALL}-*EST1* strain contained the *tlc1-tm* allele. This strain was then transformed
470 with a PCR product containing the wild-type *TLC1* allele and immediately grown on media
471 containing glucose, which shut off expression of *EST1*. Successfully transformed cells were
472 cultured in YPD media and eventually arrested in late G1 phase by the addition of alpha
473 factor (Sigma-Aldrich). Cells were washed and resuspended in YPGal to induce the

474 expression of wild-type telomerase, allowing the extension of *tlc1-tm* mutant telomeres
475 during a single cell division.
476
477 **Liquid culture senescence assay**
478 Senescence assays in liquid culture were performed essentially as previously described (van
479 Mourik et al., 2016).
480
481 **TERRA and URA3 level analysis by quantitative reverse transcription and PCR**
482 TERRA levels were measured essentially as previously described (Graf et al., 2017), while
483 URA3 and ACT1 levels were measured by one-step RT-PCR with specific primers
484 (Supplementary Table S3) following the standard protocol of the RNeasy® Mini kit
485 (Qiagen). All strains were propagated for at least 100 generations before analysis.
486

487 Data availability

488 All data generated or analyzed during this study are included in this published article (and its
489 supplementary information files).
490

491 Acknowledgments

492 We thank K. Paeschke and L. Wanders for critical reading of the manuscript; S. Pandey and
493 O. Rosas Bringas for help with data analysis; and H.G. Kazemier for technical assistance.
494 F.R.R.B. was supported by a CONACYT scholarship. S.S. was supported by an EMBO
495 Short-Term Fellowship to visit the lab of B. Luke to perform TERRA measurements and to
496 gain experience with ChIP-qPCR experiments, and we thank B. Luke and M. Graf for their
497 technical assistance. M. Cohn was supported by grants from the Carl Trygger Foundation, the
498 Erik Philip-Sörensen Foundation, and the Royal Physiographic Society in Lund. Work in the

laboratory of M. Chang was supported by a Vidi grant from the Netherlands Organization for Scientific Research.

Author Contributions

Conceptualization, F.R.R.B., S.S., M. Chang; Investigation, F.R.R.B., S.S., P.Z., M. Cohn; Writing – Original Draft, F.R.R.B., S.S., M. Chang; Writing – Reviewing & Editing, F.R.R.B., S.S., P.Z., M. Cohn, M. Chang; Supervision, M. Chang.

Competing Interests

The authors declare no competing interests.

510 **References**

511 Alexander, M. K., & Zakian, V. A. (2003, Apr 1). Rap1p telomere association is not required
512 for mitotic stability of a C_3TA_2 telomere in yeast. *EMBO J, 22*(7), 1688-1696.
513 https://doi.org/10.1093/emboj/cdg154
514

515 Aparicio, O. M., Billington, B. L., & Gottschling, D. E. (1991, Sep 20). Modifiers of position
516 effect are shared between telomeric and silent mating-type loci in *S. cerevisiae*
517 [Research Support, Non-U.S. Gov't
518 Research Support, U.S. Gov't, Non-P.H.S.
519 Research Support, U.S. Gov't, P.H.S.]. *Cell, 66*(6), 1279-1287.
520 http://www.ncbi.nlm.nih.gov/pubmed/1913809
521

522 Askree, S. H., Yehuda, T., Smolikov, S., Gurevich, R., Hawk, J., Coker, C., Krauskopf, A.,
523 Kupiec, M., & McEachern, M. J. (2004, Jun 08). A genome-wide screen for
524 *Saccharomyces cerevisiae* deletion mutants that affect telomere length. *Proc Natl*
525 *Acad Sci U S A, 101*(23), 8658-8663. https://doi.org/10.1073/pnas.0401263101
526

527 Azad, G. K., & Tomar, R. S. (2016, Jun 1). The multifunctional transcription factor Rap1: a
528 regulator of yeast physiology. *Front Biosci (Landmark Ed), 21*, 918-930.
529 https://doi.org/10.2741/4429
530

531 Berthiau, A. S., Yankulov, K., Bah, A., Revardel, E., Luciano, P., Wellinger, R. J., Geli, V.,
532 & Gilson, E. (2006, Feb 22). Subtelomeric proteins negatively regulate telomere
533 elongation in budding yeast. *EMBO J, 25*(4), 846-856.
534 https://doi.org/10.1038/sj.emboj.7600975
535

536 Bonetti, D., Clerici, M., Anbalagan, S., Martina, M., Lucchini, G., & Longhese, M. P.
537 (2010a). Shelterin-like proteins and Yku inhibit nucleolytic processing of
538 *Saccharomyces cerevisiae* telomeres. *PLoS Genet, 6*(5), e1000966.
539 https://doi.org/10.1371/journal.pgen.1000966
540

541 Bonetti, D., Clerici, M., Manfrini, N., Lucchini, G., & Longhese, M. P. (2010b, Nov 30). The
542 MRX complex plays multiple functions in resection of Yku- and Rif2-protected DNA
543 ends. *PLoS One, 5*(11), e14142. https://doi.org/10.1371/journal.pone.0014142
544

545 Bonetti, D., Martina, M., Clerici, M., Lucchini, G., & Longhese, M. P. (2009, Jul 10).
546 Multiple pathways regulate 3' overhang generation at *S. cerevisiae* telomeres. *Mol*
547 *Cell, 35*(1), 70-81. https://doi.org/10.1016/j.molcel.2009.05.015
548

549 Brevet, V., Berthiau, A. S., Civitelli, L., Donini, P., Schramke, V., Geli, V., Ascenzioni, F., &
550 Gilson, E. (2003, Apr 1). The number of vertebrate repeats can be regulated at yeast

551 telomeres by Rap1-independent mechanisms. *EMBO J, 22*(7), 1697-1706.
552 https://doi.org/10.1093/emboj/cdg155
553

554 Brigati, C., Kurtz, S., Balderes, D., Vidali, G., & Shore, D. (1993, Feb). An essential yeast
555 gene encoding a TTAGGG repeat-binding protein. *Mol Cell Biol, 13*(2), 1306-1314.
556 https://doi.org/10.1128/mcb.13.2.1306
557

558 Buchman, A. R., Kimmerly, W. J., Rine, J., & Kornberg, R. D. (1988, Jan). Two DNA-
559 binding factors recognize specific sequences at silencers, upstream activating
560 sequences, autonomously replicating sequences, and telomeres in *Saccharomyces*
561 *cerevisiae*. *Mol Cell Biol, 8*(1), 210-225. https://doi.org/10.1128/mcb.8.1.210
562

563 Cassani, C., Gobbini, E., Wang, W., Niu, H., Clerici, M., Sung, P., & Longhese, M. P. (2016,
564 Feb). Tel1 and Rif2 Regulate MRX Functions in End-Tethering and Repair of DNA
565 Double-Strand Breaks. *PLoS Biol, 14*(2), e1002387.
566 https://doi.org/10.1371/journal.pbio.1002387
567

568 Chan, S. W., Chang, J., Prescott, J., & Blackburn, E. H. (2001, Aug 21). Altering telomere
569 structure allows telomerase to act in yeast lacking ATM kinases. *Curr Biol, 11*(16),
570 1240-1250. https://doi.org/10.1016/s0960-9822(01)00391-8
571

572 Chang, M., Arneric, M., & Lingner, J. (2007, Oct 1). Telomerase repeat addition processivity
573 is increased at critically short telomeres in a Tel1-dependent manner in
574 *Saccharomyces cerevisiae*. *Genes & Development, 21*(19), 2485-2494.
575 https://doi.org/10.1101/gad.1588807
576

577 Claussin, C., & Chang, M. (2015). The many facets of homologous recombination at
578 telomeres. *Microbial Cell, 2*(9), 308-321. https://doi.org/10.15698/mic2015.09.224
579

580 Conrad, M. N., Wright, J. H., Wolf, A. J., & Zakian, V. A. (1990, Nov 16). RAP1 protein
581 interacts with yeast telomeres in vivo: overproduction alters telomere structure and
582 decreases chromosome stability. *Cell, 63*(4), 739-750. https://doi.org/10.1016/0092-
583 8674(90)90140-a
584

585 Cooper, J. P., Nimmo, E. R., Allshire, R. C., & Cech, T. R. (1997, Feb 20). Regulation of
586 telomere length and function by a Myb-domain protein in fission yeast. *Nature,*
587 *385*(6618), 744-747.
588 http://www.ncbi.nlm.nih.gov/entrez/query.fcgi?cmd=Retrieve&db=PubMed&dopt=C
589 itation&list_uids=9034194
590

591 Craven, R. J., & Petes, T. D. (1999, Aug). Dependence of the regulation of telomere length
592 on the type of subtelomeric repeat in the yeast *Saccharomyces cerevisiae*. *Genetics,*

593 *152*(4), 1531-1541.
594 http://www.ncbi.nlm.nih.gov/entrez/query.fcgi?cmd=Retrieve&db=PubMed&dopt=C
595 itation&list_uids=10430581
596

597 de Lange, T. (2018, Nov 23). Shelterin-Mediated Telomere Protection. *Annual Review of*
598 *Genetics, 52*, 223-247. https://doi.org/10.1146/annurev-genet-032918-021921
599

600 Douglas, M. E., & Diffley, J. F. X. (2021, Jun 4). Budding yeast Rap1, but not telomeric
601 DNA, is inhibitory for multiple stages of DNA replication in vitro. *Nucleic Acids Res,*
602 *49*(10), 5671-5683. https://doi.org/10.1093/nar/gkab416
603

604 Eldridge, A. M., Halsey, W. A., & Wuttke, D. S. (2006, Jan 24). Identification of the
605 determinants for the specific recognition of single-strand telomeric DNA by Cdc13.
606 *Biochemistry, 45*(3), 871-879. https://doi.org/10.1021/bi0512703
607

608 Förstemann, K., & Lingner, J. (2001, Nov). Molecular basis for telomere repeat divergence in
609 budding yeast. *Mol Cell Biol, 21*(21), 7277-7286.
610 http://www.ncbi.nlm.nih.gov/entrez/query.fcgi?cmd=Retrieve&db=PubMed&dopt=C
611 itation&list_uids=11585910
612

613 Förstemann, K., Zaug, A. J., Cech, T. R., & Lingner, J. (2003, Mar 15). Yeast telomerase is
614 specialized for C/A-rich RNA templates. *Nucleic Acids Res, 31*(6), 1646-1655.
615 http://www.ncbi.nlm.nih.gov/entrez/query.fcgi?cmd=Retrieve&db=PubMed&dopt=C
616 itation&list_uids=12626706
617

618 Gartenberg, M. R., & Smith, J. S. (2016, Aug). The Nuts and Bolts of Transcriptionally
619 Silent Chromatin in *Saccharomyces cerevisiae*. *Genetics, 203*(4), 1563-1599.
620 https://doi.org/10.1534/genetics.112.145243
621

622 Garvik, B., Carson, M., & Hartwell, L. (1995, Nov). Single-stranded DNA arising at
623 telomeres in *cdc13* mutants may constitute a specific signal for the *RAD9* checkpoint.
624 *Mol Cell Biol, 15*(11), 6128-6138.
625 http://www.ncbi.nlm.nih.gov/entrez/query.fcgi?cmd=Retrieve&db=PubMed&dopt=C
626 itation&list_uids=7565765
627

628 Gottschling, D. E., Aparicio, O. M., Billington, B. L., & Zakian, V. A. (1990). Position effect
629 at *S. cerevisiae* telomeres: Reversible repression of Pol II transcription. *Cell, 63*, 751-
630 762. https://doi.org/10.1016/0092-8674(90)90141-Z
631

632 Graf, M., Bonetti, D., Lockhart, A., Serhal, K., Kellner, V., Maicher, A., Jolivet, P., Teixeira,
633 M. T., & Luke, B. (2017, Jun 29). Telomere Length Determines TERRA and R-Loop

Regulation through the Cell Cycle. *Cell, 170*(1), 72-85 e14. https://doi.org/10.1016/j.cell.2017.06.006

Graham, I. R., & Chambers, A. (1994). Use of a selection technique to identify the diversity of binding sites for the yeast RAP1 transcription factor. *Nucleic Acids Research, 22*, 124-130.

Grandin, N., Damon, C., & Charbonneau, M. (2001, Mar 1). Ten1 functions in telomere end protection and length regulation in association with Stn1 and Cdc13. *EMBO J, 20*(5), 1173-1183. https://doi.org/10.1093/emboj/20.5.1173

Grandin, N., Reed, S. I., & Charbonneau, M. (1997, Feb 15). Stn1, a new *Saccharomyces cerevisiae protein*, is implicated in telomere size regulation in association with Cdc13. *Genes Dev, 11*(4), 512-527. http://www.ncbi.nlm.nih.gov/entrez/query.fcgi?cmd=Retrieve&db=PubMed&dopt=Citation&list_uids=9042864

Gravel, S., Larrivee, M., Labrecque, P., & Wellinger, R. J. (1998, May 1). Yeast Ku as a regulator of chromosomal DNA end structure. *Science, 280*(5364), 741-744. http://www.ncbi.nlm.nih.gov/entrez/query.fcgi?cmd=Retrieve&db=PubMed&dopt=Citation&list_uids=9563951

Grossi, S., Bianchi, A., Damay, P., & Shore, D. (2001, Dec). Telomere formation by Rap1p binding site arrays reveals end-specific length regulation requirements and active telomeric recombination. *Mol Cell Biol, 21*(23), 8117-8128. https://doi.org/10.1128/MCB.21.23.8117-8128.2001

Guérin, T. M., Béneut, C., Barinova, N., López, V., Lazar-Stefanita, L., Deshayes, A., Thierry, A., Koszul, R., Dubrana, K., & Marcand, S. (2019, Jul 11). Condensin-Mediated Chromosome Folding and Internal Telomeres Drive Dicentric Severing by Cytokinesis. *Mol Cell, 75*(1), 131-144 e133. https://doi.org/10.1016/j.molcel.2019.05.021

Hailemariam, S., De Bona, P., Galletto, R., Hohl, M., Petrini, J. H., & Burgers, P. M. (2019, Dec 6). The telomere-binding protein Rif2 and ATP-bound Rad50 have opposing roles in the activation of yeast Tel1(ATM) kinase. *J Biol Chem, 294*(49), 18846-18852. https://doi.org/10.1074/jbc.RA119.011077

Hardy, C. F., Sussel, L., & Shore, D. (1992, May). A RAP1-interacting protein involved in transcriptional silencing and telomere length regulation. *Genes Dev, 6*(5), 801-814. http://www.ncbi.nlm.nih.gov/entrez/query.fcgi?cmd=Retrieve&db=PubMed&dopt=Citation&list_uids=1577274

677 Hass, E. P., & Zappulla, D. C. (2015, Jul 28). The Ku subunit of telomerase binds Sir4 to
678 recruit telomerase to lengthen telomeres in *S. cerevisiae*. *eLife, 4*.
679 https://doi.org/10.7554/eLife.07750
680

681 Hirano, Y., Fukunaga, K., & Sugimoto, K. (2009, Feb 13). Rif1 and Rif2 inhibit localization
682 of Tel1 to DNA ends. *Mol Cell, 33*(3), 312-322. https://doi.org/S1097-
683 2765(09)00024-0 [pii]
684 10.1016/j.molcel.2008.12.027
685

686 Iglesias, N., Redon, S., Pfeiffer, V., Dees, M., Lingner, J., & Luke, B. (2011, Jun).
687 Subtelomeric repetitive elements determine TERRA regulation by Rap1/Rif and
688 Rap1/Sir complexes in yeast. *EMBO Rep, 12*(6), 587-593.
689 https://doi.org/10.1038/embor.2011.73
690

691 Khayat, F., Cannavo, E., Alshmery, M., Foster, W. R., Chahwan, C., Maddalena, M., Smith,
692 C., Oliver, A. W., Watson, A. T., Carr, A. M., Cejka, P., & Bianchi, A. (2021, Jun
693 22). Inhibition of MRN activity by a telomere protein motif. *Nat Commun, 12*(1),
694 3856. https://doi.org/10.1038/s41467-021-24047-2
695

696 Krauskopf, A., & Blackburn, E. H. (1996, Sep 26). Control of telomere growth by
697 interactions of RAP1 with the most distal telomeric repeats. *Nature, 383*(6598), 354-
698 357. https://doi.org/10.1038/383354a0
699

700 Kyrion, G., Liu, K., Liu, C., & Lustig, A. J. (1993, Jul). RAP1 and telomere structure
701 regulate telomere position effects in *Saccharomyces cerevisiae*. *Genes Dev, 7*(7A),
702 1146-1159. https://doi.org/10.1101/gad.7.7a.1146
703

704 Levy, D. L., & Blackburn, E. H. (2004, Dec). Counting of Rif1p and Rif2p on
705 *Saccharomyces cerevisiae* telomeres regulates telomere length. *Mol Cell Biol, 24*(24),
706 10857-10867. https://doi.org/24/24/10857 [pii]
707 10.1128/MCB.24.24.10857-10867.2004
708

709 Lieb, J. D., Liu, X., Botstein, D., & Brown, P. O. (2001, Aug). Promoter-specific binding of
710 Rap1 revealed by genome-wide maps of protein-DNA association. *Nat Genet, 28*(4),
711 327-334. https://doi.org/10.1038/ng569
712

713 Lin, J., Smith, D. L., & Blackburn, E. H. (2004, Apr). Mutant telomere sequences lead to
714 impaired chromosome separation and a unique checkpoint response. *Mol Biol Cell,*
715 *15*(4), 1623-1634.
716 http://www.ncbi.nlm.nih.gov/entrez/query.fcgi?cmd=Retrieve&db=PubMed&dopt=C
717 itation&list_uids=14742705
718

Lingner, J., Hughes, T. R., Shevchenko, A., Mann, M., Lundblad, V., & Cech, T. R. (1997, Apr 25). Reverse transcriptase motifs in the catalytic subunit of telomerase. *Science, 276*(5312), 561-567. http://www.ncbi.nlm.nih.gov/entrez/query.fcgi?cmd=Retrieve&db=PubMed&dopt=Citation&list_uids=9110970

Lundblad, V., & Blackburn, E. H. (1993, Apr 23). An alternative pathway for yeast telomere maintenance rescues *est1*- senescence. *Cell, 73*(2), 347-360. https://doi.org/0092-8674(93)90234-H [pii]

Lundblad, V., & Struhl, K. (2010). Yeast. *Current Protocols in Molecular Biology, 92*(1). https://doi.org/10.1002/0471142727.mb1300s92

Lustig, A. J., Kurtz, S., & Shore, D. (1990, Oct 26). Involvement of the silencer and UAS binding protein RAP1 in regulation of telomere length. *Science, 250*(4980), 549-553.

Makovets, S., Herskowitz, I., & Blackburn, E. H. (2004, May). Anatomy and dynamics of DNA replication fork movement in yeast telomeric regions. *Mol Cell Biol, 24*(9), 4019-4031. http://www.ncbi.nlm.nih.gov/entrez/query.fcgi?cmd=Retrieve&db=PubMed&dopt=Citation&list_uids=15082794

Marcand, S., Gilson, E., & Shore, D. (1997, Feb 14). A protein-counting mechanism for telomere length regulation in yeast [Research Support, Non-U.S. Gov't Research Support, U.S. Gov't, P.H.S.]. *Science, 275*(5302), 986-990. http://www.ncbi.nlm.nih.gov/pubmed/9020083

Marcand, S., Pardo, B., Gratias, A., Cahun, S., & Callebaut, I. (2008, May 1). Multiple pathways inhibit NHEJ at telomeres. *Genes Dev, 22*(9), 1153-1158. https://doi.org/10.1101/gad.455108

Marsella, A., Gobbini, E., Cassani, C., Tisi, R., Cannavo, E., Reginato, G., Cejka, P., & Longhese, M. P. (2021, Mar 30). Sae2 and Rif2 regulate MRX endonuclease activity at DNA double-strand breaks in opposite manners. *Cell Rep, 34*(13), 108906. https://doi.org/10.1016/j.celrep.2021.108906

Moretti, P., Freeman, K., Coodly, L., & Shore, D. (1994, Oct 1). Evidence that a complex of SIR proteins interacts with the silencer and telomere-binding protein RAP1. *Genes Dev, 8*(19), 2257-2269. https://www.ncbi.nlm.nih.gov/pubmed/7958893

759 Negrini, S., Ribaud, V., Bianchi, A., & Shore, D. (2007). DNA breaks are masked by
760 multiple Rap1 binding in yeast: Implications for telomere capping and telomerase
761 regulation. *Genes & Development, 21*, 292-302. https://doi.org/10.1101/gad.400907
762

763 Nugent, C. I., Hughes, T. R., Lue, N. F., & Lundblad, V. (1996, Oct 11). Cdc13p: a single-
764 strand telomeric DNA-binding protein with a dual role in yeast telomere maintenance.
765 *Science, 274*(5285), 249-252.
766 http://www.ncbi.nlm.nih.gov/entrez/query.fcgi?cmd=Retrieve&db=PubMed&dopt=C
767 itation&list_uids=8824190
768

769 Oh, J., & Symington, L. S. (2018, Nov 29). Role of the Mre11 Complex in Preserving
770 Genome Integrity. *Genes (Basel), 9*(12). https://doi.org/10.3390/genes9120589
771

772 Pardo, B., & Marcand, S. (2005, Sep 07). Rap1 prevents telomere fusions by nonhomologous
773 end joining. *EMBO J, 24*(17), 3117-3127. https://doi.org/10.1038/sj.emboj.7600778
774

775 Paschini, M., Toro, T. B., Lubin, J. W., Braunstein-Ballew, B., Morris, D. K., & Lundblad,
776 V. (2012, May). A naturally thermolabile activity compromises genetic analysis of
777 telomere function in *Saccharomyces cerevisiae*. *Genetics, 191*(1), 79-93.
778 https://doi.org/10.1534/genetics.111.137869
779

780 Prescott, J. C., & Blackburn, E. H. (2000, Apr). Telomerase RNA template mutations reveal
781 sequence-specific requirements for the activation and repression of telomerase action
782 at telomeres. *Mol Cell Biol, 20*(8), 2941-2948. https://doi.org/10.1128/mcb.20.8.2941-
783 2948.2000
784

785 Preti, M., Ribeyre, C., Pascali, C., Bosio, M. C., Cortelazzi, B., Rougemont, J., Guarnera, E.,
786 Naef, F., Shore, D., & Dieci, G. (2010, May 28). The telomere-binding protein Tbf1
787 demarcates snoRNA gene promoters in *Saccharomyces cerevisiae*. *Mol Cell, 38*(4),
788 614-620. https://doi.org/10.1016/j.molcel.2010.04.016
789

790 Roisné-Hamelin, F., Pobiega, S., Jézéquel, K., Miron, S., Dépagne, J., Veaute, X., Busso, D.,
791 Du, M. L., Callebaut, I., Charbonnier, J. B., Cuniasse, P., Zinn-Justin, S., & Marcand,
792 S. (2021, May 12). Mechanism of MRX inhibition by Rif2 at telomeres. *Nat*
793 *Commun, 12*(1), 2763. https://doi.org/10.1038/s41467-021-23035-w
794

795 Rossmann, M. P., Luo, W., Tsaponina, O., Chabes, A., & Stillman, B. (2011, Apr 8). A
796 common telomeric gene silencing assay is affected by nucleotide metabolism. *Mol*
797 *Cell, 42*(1), 127-136. https://doi.org/10.1016/j.molcel.2011.03.007
798

799 Sabourin, M., Tuzon, C. T., & Zakian, V. A. (2007, Jul 24). Telomerase and Tel1p
800 Preferentially Associate with Short Telomeres in *S. cerevisiae*. *Mol Cell*.

http://www.ncbi.nlm.nih.gov/entrez/query.fcgi?cmd=Retrieve&db=PubMed&dopt=Citation&list_uids=17656141

Sandell, L. L., & Zakian, V. A. (1993, Nov 19). Loss of a yeast telomere: arrest, recovery, and chromosome loss. *Cell, 75*(4), 729-739. https://www.ncbi.nlm.nih.gov/pubmed/8242745

Shampay, J., Szostak, J. W., & Blackburn, E. H. (1984). DNA sequences of telomeres maintained in yeast. *Nature, 310*, 154-157. https://doi.org/10.1038/310154a0

Sherman, F. (2002). Getting started with yeast. *Methods Enzymol, 350*, 3-41. https://www.ncbi.nlm.nih.gov/pubmed/12073320

Shi, T., Bunker, R. D., Mattarocci, S., Ribeyre, C., Faty, M., Gut, H., Scrima, A., Rass, U., Rubin, S. M., Shore, D., & Thoma, N. H. (2013, Jun 6). Rif1 and Rif2 shape telomere function and architecture through multivalent Rap1 interactions. *Cell, 153*(6), 1340-1353. https://doi.org/10.1016/j.cell.2013.05.007

Shore, D., & Nasmyth, K. (1987, Dec 4). Purification and cloning of a DNA binding protein from yeast that binds to both silencer and activator elements [Research Support, Non-U.S. Gov't]. *Cell, 51*(5), 721-732. http://www.ncbi.nlm.nih.gov/pubmed/3315231

Steinberg-Neifach, O., & Lue, N. F. (2015). Telomere DNA recognition in Saccharomycotina yeast: potential lessons for the co-evolution of ssDNA and dsDNA-binding proteins and their target sites. *Front Genet, 6*, 162. https://doi.org/10.3389/fgene.2015.00162

Stinus, S., Paeschke, K., & Chang, M. (2017, Oct 20). Telomerase regulation by the Pif1 helicase: a length-dependent effect? *Curr Genet*. https://doi.org/10.1007/s00294-017-0768-6

Strecker, J., Stinus, S., Caballero, M. P., Szilard, R. K., Chang, M., & Durocher, D. (2017, Aug 03). A sharp Pif1-dependent threshold separates DNA double-strand breaks from critically short telomeres. *eLife, 6*, e23783. https://doi.org/10.7554/eLife.23783

Symington, L. S., Rothstein, R., & Lisby, M. (2014, Nov). Mechanisms and Regulation of Mitotic Recombination in *Saccharomyces cerevisiae*. *Genetics, 198*(3), 795-835. https://doi.org/10.1534/genetics.114.166140

Teixeira, M. T., Arneric, M., Sperisen, P., & Lingner, J. (2004, Apr 30). Telomere length homeostasis is achieved via a switch between telomerase- extendible and -nonextendible states. *Cell, 117*(3), 323-335.

842 http://www.ncbi.nlm.nih.gov/entrez/query.fcgi?cmd=Retrieve&db=PubMed&dopt=C
843 itation&list_uids=15109493
844

845 Teng, S. C., & Zakian, V. A. (1999, Dec). Telomere-telomere recombination is an efficient
846 bypass pathway for telomere maintenance in *Saccharomyces cerevisiae*. *Mol Cell*
847 *Biol, 19*(12), 8083-8093.
848 http://www.ncbi.nlm.nih.gov/entrez/query.fcgi?cmd=Retrieve&db=PubMed&dopt=C
849 itation&list_uids=10567534
850

851 van Mourik, P. M., de Jong, J., Agpalo, D., Claussin, C., Rothstein, R., & Chang, M. (2016).
852 Recombination-Mediated Telomere Maintenance in *Saccharomyces cerevisiae* Is Not
853 Dependent on the Shu Complex. *PLoS One, 11*(3), e0151314.
854 https://doi.org/10.1371/journal.pone.0151314
855

856 van Mourik, P. M., de Jong, J., Sharma, S., Kavsek, A., Chabes, A., & Chang, M. (2018, Jul
857 31). Upregulation of dNTP Levels After Telomerase Inactivation Influences
858 Telomerase-Independent Telomere Maintenance Pathway Choice in *Saccharomyces*
859 *cerevisiae*. *G3 (Bethesda), 8*(8), 2551-2558. https://doi.org/10.1534/g3.118.200280
860

861 Vodenicharov, M. D., Laterreur, N., & Wellinger, R. J. (2010, Sep 1). Telomere capping in
862 non-dividing yeast cells requires Yku and Rap1. *EMBO J, 29*(17), 3007-3019.
863 https://doi.org/10.1038/emboj.2010.155
864

865 Wahlin, J., & Cohn, M. (2000). *Saccharomyces cerevisiae* RAP1 binds to telomeric
866 sequences with spatial flexibility. *Nucleic Acids Research, 28*, 2292-2301.
867 https://doi.org/10.1093/nar/28.12.2292
868

869 Wellinger, R. J. (2014, Mar 20). In the end, what's the problem? *Mol Cell, 53*(6), 855-856.
870 https://doi.org/10.1016/j.molcel.2014.03.008
871

872 Wellinger, R. J., & Zakian, V. A. (2012, Aug). Everything you ever wanted to know about
873 *Saccharomyces cerevisiae* telomeres: beginning to end [Research Support, N.I.H.,
874 Extramural
875 Research Support, Non-U.S. Gov't
876 Review]. *Genetics, 191*(4), 1073-1105. https://doi.org/10.1534/genetics.111.137851
877

878 Wilson, T. E., Grawunder, U., & Lieber, M. R. (1997, Jul 31). Yeast DNA ligase IV mediates
879 non-homologous DNA end joining. *Nature, 388*(6641), 495-498.
880 https://doi.org/10.1038/41365
881

882 Wotton, D., & Shore, D. (1997, Mar 15). A novel Rap1p-interacting factor, Rif2p, cooperates
883 with Rif1p to regulate telomere length in *Saccharomyces cerevisiae*. *Genes Dev,*

11(6), 748-760.
http://www.ncbi.nlm.nih.gov/entrez/query.fcgi?cmd=Retrieve&db=PubMed&dopt=Citation&list_uids=9087429

889 **Figure Legends**

890

891 **Figure 1. Rap1 binds poorly to *tlc1-tm* telomere sequences**

892 (A) Exponentially growing cells of the indicated genotypes were diluted to an OD_{600} of 0.05
893 and monitored for 8 h. Three clones of each genotype were followed, and the average of the
894 measurements at each time point is plotted. Error bars are too small to be visualized.

895 (B) Telomere Southern blot analysis of *TLC1* and *tlc1-tm* cells (three clonal isolates per
896 genotype). Black arrowhead indicates a 1.8 kb DNA fragment generated from the BsmAI-
897 digestion of plasmid pYt103 (Shampay et al., 1984). The major terminal restriction fragment
898 is below the 1.8 kb control band.

899 (C) Southern blot analysis of the artificial VII-L telomere, with either wild-type or *tlc1-tm*
900 mutant sequence, using a probe to the adjacent *URA3* gene. Multiple clones were examined,
901 with each clone propagated for 1 to 4 passages (each passage corresponds to approximately
902 25 generations). A wild-type strain (lacking the artificial VII-L telomere) was used as a
903 control.

904 (D, F, G) ChIP-qPCR analysis of the association of (D) Protein A-tagged Rap1, (F) Myc-
905 tagged Cdc13, and (G) Myc-tagged Tbf1 to six Y′ telomeres, the VII-L telomere, or to the
906 non-telomeric *ARO1* locus. Untagged wild-type and *tlc1-tm* strains were used as controls.
907 The mean percentage of input ±SEM is shown (n=3, ** $p<0.01$).

908 (E) EMSA of Rap1 protein incubated with radiolabeled oligonucleotides with either wild-
909 type or *tlc1-tm* mutant telomeric sequence.

910

911 **Figure 2. Telomere length regulation is disrupted in *tlc1-tm* cells**

912 (A) Southern blot analysis of the artificial VII-L telomere using a probe to the adjacent *URA3*
913 gene. The telomere was seeded with either wild-type or *tlc1-tm* mutant sequence of the

914 indicated lengths in a strain expressing wild-type TLC1. Multiple clones of each strain were
915 examined. A wild-type strain (lacking the artificial VII-L telomere) was used as a control.
916 (B) In vivo extension of *tlc1-tm* telomeres was examined using the iSTEX assay. Telomere
917 VI-R was amplified and sequenced after the induction of wild-type telomerase. Each bar
918 represents an individual telomere. The black and red portions of each bar represent wild-type
919 and *tlc1-tm* sequence, respectively, that is identical in sequence and thus present before
920 telomerase induction. The length of the black/wild-type sequence is 48 bp. Sequence that is
921 divergent from the black and red sequence is shown in grey and green. Grey represents newly
922 added wild-type sequence after the induction of telomerase. Green represents divergent *tlc1-*
923 *tm* sequence, most likely a result of homologous recombination. Telomeres are sorted based
924 on the length of the undiverged (black plus red) sequence.
925 (C) Telomere VI-R sequences obtained from the iSTEX analysis in B were binned into
926 groups of 10 nt in size according to telomere length before telomerase induction. iSTEX data
927 for the extension of wild-type telomeres were taken from previous studies (Strecker et al.,
928 2017; Stinus et al., 2017) and included for comparison. Groups containing less than four
929 telomeres were excluded from this analysis. Frequency of extension and average telomere
930 length before telomerase induction were calculated and plotted for each group. Logarithmic
931 regression curves for each data set were also included in the plot. Telomeres shorter than 40
932 nt before telomerase induction, which are not efficiently recognized and extended by
933 telomerase (Strecker et al., 2017), were removed from the regression analysis.
934
935 **Figure 3. Fast degradation of *tlc1-tm* telomeres in the absence of telomerase**
936 (A) Senescence rates were measured by serial passaging of strains of the indicated genotypes,
937 derived from the sporulation of *est2Δ/EST2* and *est2Δ/EST2 tlc1-tm/tlc1-tm* diploids (top
938 panel) or *tlc1Δ/TLC1* and *tlc1Δ/tlc1-tm* diploids (bottom panel). Cell density was measured

939 every 24 h, followed by dilution to $1x10^5$ cell/ml. Mean ±SEM of four independent isolates
940 per genotype is plotted.
941 (B) Telomere Southern blot analysis of samples obtained at the first time point of the
942 senescence assays in A. Black arrowhead indicates the 1.8 kb telomere sequence-containing
943 fragment loaded as control, as in Figure 1B.
944
945 **Figure 4. Recruitment of Rif1 and Sir4, but not Rif2 nor Sir3, is significantly reduced at**
946 ***tlc1-tm* telomeres**
947 (A) ChIP-qPCR analysis of the association of Myc-tagged Rif1, Rif2, Sir4, and Protein A-
948 tagged Sir3 to six Y′ telomeres, the VII-L telomere, or to the non-telomeric *ARO1* locus.
949 Untagged wild-type and *tlc1-tm* strains were used as controls.
950 (B) Total RNA was reverse transcribed and TERRA from specific telomeres (I-L and XV-L)
951 was analyzed by qPCR. TERRA values were normalized to ACT1 levels, and to the
952 respective wild type (*TLC1*).
953 (C) Tenfold serial dilutions of strains with the indicated genotypes were spotted on SC plates
954 without or with 5-FOA.
955 (D) The expression of the subtelomerically integrated *URA3* gene was measured in the
956 indicated yeast strains by RT-qPCR.
957 All data (except C) are shown as mean ±SEM (n=3, *** $p<10^{-3}$, **** $p<10^{-4}$).
958
959 **Figure 5. Rif2 prevents degradation of *tlc1-tm* telomeres**
960 (A-C) Telomere Southern blot analysis of strains of the indicated genotypes. Black
961 arrowhead indicates the 1.8 kb telomere sequence-containing fragment loaded as control, as
962 in Figure 1B.

963 (D) Colony sizes of haploid meiotic progeny derived from the sporulation of *rad52Δ/RAD52*
964 *rif2Δ/RIF2* and *rad52Δ/RAD52 rif2Δ/RIF2 tlc1-tm/tlc1-tm* diploid strains were measured and
965 normalized to wild-type (top panel) or *tlc1-tm* (bottom panel). The number of colonies
966 analyzed is indicated in parenthesis. Error bars show SEM.
967 (E) Tenfold serial dilutions of strains with the indicated genotypes were spotted on YPD
968 plates and grown at 30ºC.
969
970 **Figure 6. Rif2 protects *tlc1-tm* telomeres by inhibiting the MRX complex and acts in**
971 **parallel with the Yku complex**
972 (A&C) ChIP-qPCR analysis of the association of Myc-tagged Mre11 and Yku70 to six Y′
973 telomeres, the VII-L telomere, or to the non-telomeric *ARO1* locus. Untagged wild-type and
974 *tlc1-tm* strains were used as controls. The mean percentage of input ±SEM is shown (n=3, **
975 p<0.01).
976 (B&D) Telomere Southern blot analysis of strains of the indicated genotypes. Black
977 arrowhead indicates the 1.8 kb telomere sequence-containing fragment loaded as control, as
978 in Figure 1B. (B) Parental diploid 1 is *rad50Δ/RAD50 rif2Δ/RIF2*; parental diploid 2 is
979 *rad50Δ/RAD50 rif2Δ/RIF2 tlc1-tm/tlc1-tm*. The last six lanes are derived from cells grown at
980 22°C. (D) Parental diploid 1 is *exo1Δ/EXO1 yku70Δ/YKU70*; parental diploid 2 is
981 *exo1Δ/EXO1 yku70Δ/YKU70 tlc1-tm/tlc1-tm*.
982 (E) Colony sizes of haploid meiotic progeny derived from the sporulation of *rif2Δ/RIF2*
983 *yku70Δ/YKU70* and *rif2Δ/RIF2 yku70Δ/YKU70 tlc1-tm/tlc1-tm* diploid strains were measured
984 and normalized to wild-type (top panel) or *tlc1-tm* (bottom panel). The number of colonies
985 analyzed is indicated in parenthesis. Error bars show SEM. Representative images of
986 dissected tetrads are shown on the right. Each column of colonies arose from a single tetrad.
987

988

989 **Figure 7. Rif2 association to *tlc1-tm* telomeres requires the MRX complex**

990 (A) Telomere Southern blot analysis of strains of the indicated genotypes. Black arrowhead
991 indicates the 1.8 kb telomere sequence-containing fragment loaded as control, as in Figure
992 1B.

993 (B) Colony sizes of haploid meiotic progeny derived from the sporulation of a *rif2Δ/RIF2*
994 *yku70Δ/YKU70 tlc1-476A/TLC1* diploid strain were measured and normalized to wild-type.
995 The number of colonies analyzed is indicated in parenthesis. Error bars show SEM.
996 Representative images of dissected tetrads are shown on the right. Each column of colonies
997 arose from a single tetrad.

998 (C) ChIP-qPCR analysis of the association of Myc-tagged Rif2 to a 300-bp ITS located on
999 chromosome III containing either wild-type or *tlc1-tm* sequence. The mean percentage of
1000 input ±SEM is shown (n=3, *** $p<10^{-3}$).

1001 (D) ChIP-qPCR analysis of the association of Myc-tagged Rif2 to six Y′ telomeres, the VII-L
1002 telomere, or to the non-telomeric *ARO1* locus in a *rad50Δ* background. Untagged strains
1003 were used as controls. The mean percentage of input ±SEM is shown (n=3, **** $p<10^{-4}$).

1004 **Supplemental Information**

1005

1006 Supplementary Table S1. Yeast strains used in this study.

1007 Supplementary Table S2. Wild-type and mutant sequences used to replace the VII-L

1008 telomere.

1009 Supplementary Table S3. qPCR primers.

1010 Supplementary Figure 1. Tbf1 binding motifs adjacent to the artificial VII-L telomere.

1011 Supplementary Figure 2. Rif2 protects *tlc1-tm* telomeres from degradation.

1012 Supplementary Figure 3. Slightly differences in the telomere profile of isogenic *tlc1-tm*

1013 strains are not due to Rad52-dependent homologous recombination.

1014

>adh4::URA3-VII-L-telomere

TTAATATTCATAGGCTTTCTTGATAATGGCAACCACTTGTTCTTTGGTGAATTGAACTGGGTTAGTCAAATGG
CAGGCATCATGCATGGCGTGTTCAGCCAAAATGTCAAAATCTTCGGTTTTAACACCTAAGTCTTTCAAGTTTC
TTGGAATGTTCATGGTTCTGTTTAAAACGTGCAAAGCCTTGATGGTTTCTTCTGGATCTTCTTGAGAAGCACC
GCAATGCAAGGCAATTTCACCTAATCTCTTCTTGGCCTTTGGACATTGCATGTTGGCCTCTTGAACATGAGGC
AACAAGACAGCGTTACAAACACCATGAGGCAAGTGGTAGAAACCACCAAGTTGATGAGCA**AGGGC**ATGAACAT
AACCTAGAGAAGCATTGTTGAAAGCCATACCTGCCAAGTATTCTGCGTAACACATATCAGTTCTGGCCTTCTT
GTCTTTACCGTCTTTGTATGCGGCGACCAAGCTTTTCAATTCATCATTTTTTTTTTATTCTTTTTTTTGATTT
CGGTTTCCTTGAAATTTTTTTGATTCGGTAATCTCCGAACAGAAGGAAGAACGAAGGAAGGAGCACAGACTTA
GATTGGTATATATACGCATATGTAGTGTTGAAGAAACATGAAATTGCCCAGTATTCTTAACCCAACTGCACAG
AACAAAAACCTGCAGGAAACGAAGATAAATCATGTCGAAAGCTACATATAAGGAACGTGCTGCTACTCATCCT
AGTCCTGTTGCTGCCAAGCTATTTAATATCATGCACGAAAAGCAAACAAACTTGTGTGCTTCATTGGATGTTC
GTACCACCAAGGAATTACTGGAGTTAGTTGAAGCATTAGGTCCCAAAATTTGTTTACTAAAAACACATGTGGA
TATCTTGACTGATTTTTCCATGG**AGGGC**ACAGTTAAGCCGCTAAAGGCATTATCCGCCAAGTACAATTTTTTA
CTCTTCGAAGACAGAAAATTTGCTGACATTGGTAATACAGTCAAATTGCAGTACTCTGCGGGTGTATACAGAA
TAGCAGAATGGGCAGACATTACGAATGCACACGGTGTGGTGGGCCCAGGTATTGTTAGCGGTTTGAAGCAGGC
GGCAGAAGAAGTAACAAAGGAACCTAGAGGCCTTTTGATGTTAGCAGAATTGTCATGCA**AGGGC**TCCCTATCT
ACTGGAGAATATACTA**AGGGT**ACTGTTGACATTGCGAAGAGCGACAAAGATTTTGTTATCGGCTTTATTGCTC
AAAGAGACATGGGTGGAAGAGATGAAGGTTACGATTGGTTGATTATGACACCCGGTGTGGGTTTAGATGACAA
GGGAGACGCATTGGGTCAACAGTATAGAACCGTGGATGATGTGGTCTCTACAGGATCTGACATTATTATTGTT
GGAAGAGGACTATTTGCAAAGGGAAGGGATGCTAAGGTAG**AGGGT**GAACGTTACAGAAAAGCAGGCTGGGAAG
CATATTTGAGAAGATGCGGCCAGCAAAACTAAAAAACTGTATTATAAGTAAATGCATGTATACTAAACTCACA
AATTAGAGCTTCAATTTAATTATATCAGTTATT**ACCCT**CGACGGATCCGGTGGTGTGGTG…

ADH4
URA3
Telomere
Tbf1 binding motif

Supplementary Fig. 1. Tbf1 binding motifs adjacent to the artificial VII-L telomere. The sequence immediately adjacent to the artificial VII-L telomeric repeats is shown. The truncated *ADH4* and full-length *URA3* sequences are highlighted, as well as sequences conforming to the RCCCT Tbf1 consensus binding motif.

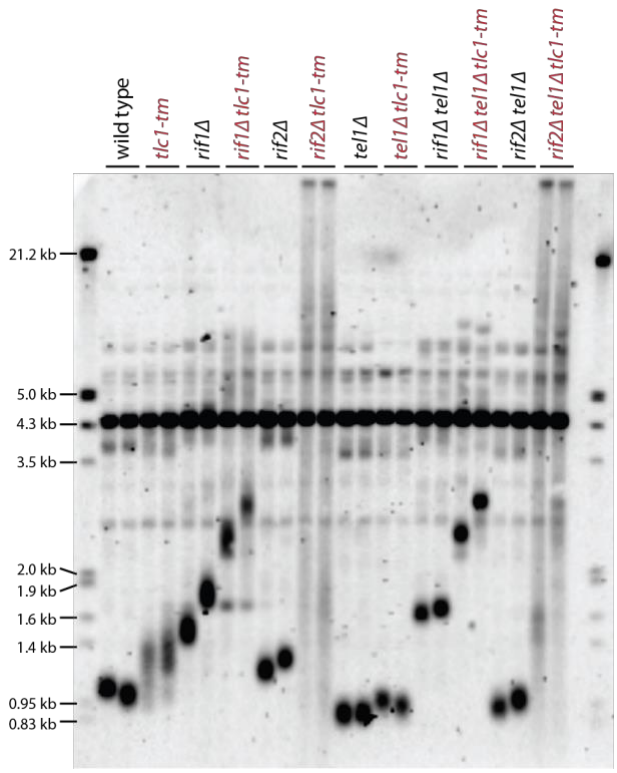

Supplementary Fig. 2. Rif2 protects *tlc1-tm* telomeres from degradation.
Southern blot analysis of the artificial VII-L telomere using a probe to the adjacent *URA3* gene in strains of the indicated genotypes.

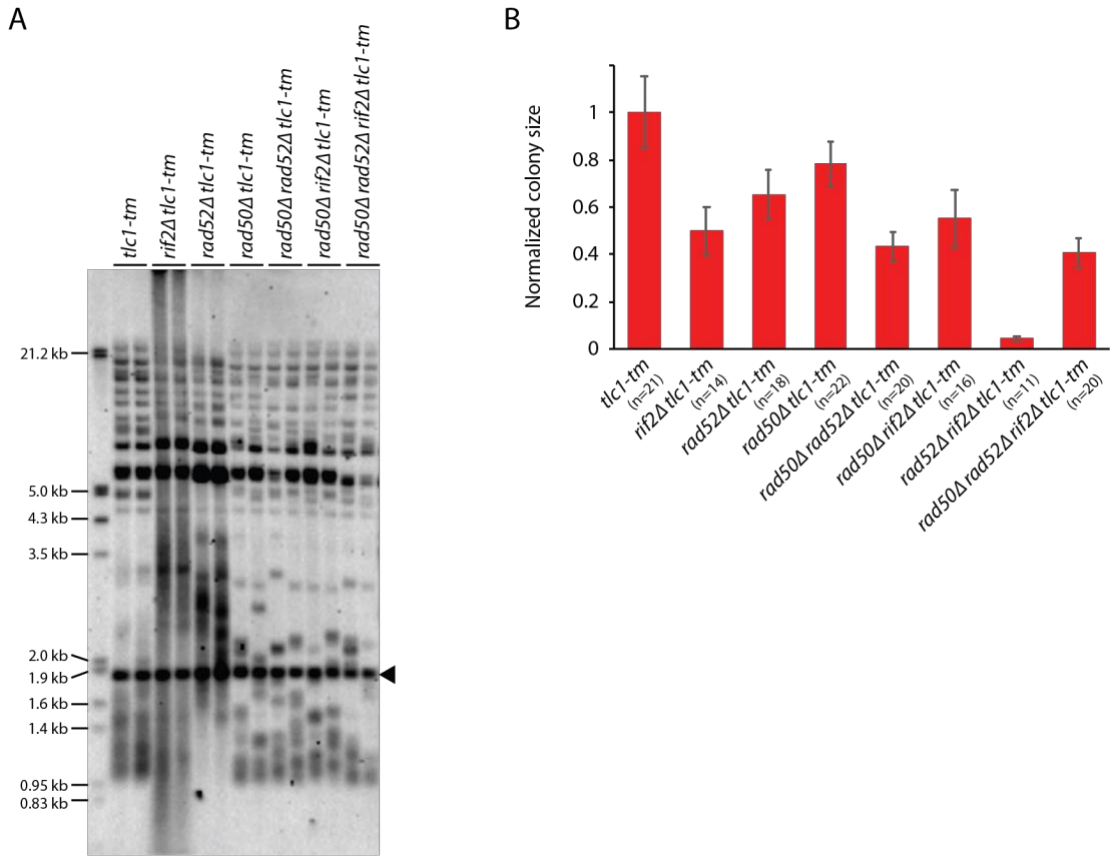

Supplementary Fig. 3. Slightly differences in the telomere profile of isogenic *tlc1-tm* strains are not due to Rad52-dependent homologous recombination.
(A) Telomere Southern blot analysis of strains of the indicated genotypes (duplicate isolates per strain). Black arrowhead indicates the 1.8 kb telomere sequence-containing fragment loaded as control, as in Figure 1B.
(B) Colony sizes of haploid meiotic progeny derived from the sporulation of a *rad50Δ/RAD50 rad52Δ/RAD52 rif2Δ/RIF2 tlc1-tm/tlc1-tm* diploid strain were measured and normalized to *tlc1-tm*. The number of colonies analyzed is indicated in parenthesis. Error bars show SEM.